NACA RM E55FO9

NACA

RESEARCH MEMORANDUM

PRELIMINARY PERFORMANCE DATA OF SEVERAL TAIL-PIPE-CASCADE-TYPE MODEL THRUST REVERSERS

By James G. Henzel, Jr., and Jack G. McArdle

Lewis Flight Propulsion Laboratory
Cleveland, Ohio

NATIONAL ADVISORY COMMITTEE
FOR AERONAUTICS

WASHINGTON

August 29, 1955

NATIONAL ADVISORY COMMITTEE FOR AERONAUTICS

RESEARCH MEMORANDUM

PRELIMINARY PERFORMANCE DATA OF SEVERAL TAIL-PIPE-CASCADE-TYPE MODEL THRUST REVERSERS

By James G. Henzel, Jr., and Jack G. McArdle

SUMMARY

The reverse-thrust performance of several tail-pipe-cascade-type model thrust reversers was obtained over a range of exhaust-nozzle pressure ratios from about 1.2 to 2.4. Both symmetrical and asymmetrical cascade blade shapes were investigated.

A thrust-reverser configuration with a symmetrical cascade-blade shape had a maximum reverse-thrust ratio of 76 percent of full forward thrust. This reverser also had good thrust-modulation characteristics. Thrust in any amount from 100 percent forward to 76 percent reverse could be obtained. In addition, the aerodynamic forces on the reverser were such that in the event of failure of an actuating linkage normal full forward thrust would be restored.

One thrust-reverser configuration with an asymmetrical cascade-blade shape and a centerbody had a reverse-thrust ratio of 88 percent of full forward thrust. A similar configuration, but without a centerbody, had a maximum reverse-thrust ratio of about 90 percent of full forward thrust.

INTRODUCTION

A research program is being conducted at the NACA Lewis laboratory to determine design criteria for thrust reversers. Thrust reversers may be desirable for controlling jet-aircraft dive velocities and to reduce jet-aircraft ground roll. Various target, ring, and cascade-type thrust reversers are being investigated. These reversers may be located either upstream or downstream of the jet-engine exhaust nozzle. References 1 and 2 reported the performance of several clam-shell and target-type thrust reversers.

This report presents preliminary data on the performance of several cascade-type thrust reversers located upstream of the exhaust nozzle. Such reversers are herein referred to as the tail-pipe-cascade type.

A total of 15 different tail-pipe-cascade configurations were investigated. These included two different blade shapes, several cascade length-to-span ratios, and various innerbody lengths. Basic reverse-thrust ratio, air-flow characteristics, and reverse-thrust ratio are plotted against exhaust-nozzle pressure ratio for all 15 configurations at full reversal. For some of the configurations, modulation performance and surveys of total pressure and flow angle were obtained at the cascade discharge.

APPARATUS AND PROCEDURE

Equipment and Instrumentation

The mechanism used to measure thrust in both positive and negative directions is shown in figure 1. The axial thrust forces along the pipe were read directly from a null-type pressure-measuring cell.

The instrumentation for the various thrust reversers is shown in figure 2. Air flow was measured by a standard ASME sharp-edged orifice. Both stationary and traversing probes were used to survey the reversers.

Reversers

The various tail-pipe-cascade-type thrust-reverser configurations are shown in figures 2 to 4 and are tabulated in table I. Both symmetrical and asymmetrical cascade-blade shapes were investigated. The symmetrical blade configurations (1 to 5) are shown in figure 2. These blades have equal entrance and exit angles and, as a result, have equal entrance and exit effective flow areas. Both thin, single curvature and thick, double curvature blades were investigated. In addition, both four- and six-bladed cascades were investigated. Reverser configurations 1 to 5 had a scheduled tail-pipe blockage. As the cascade was actuated, "duckbills" (shown in figs. 2(a), (b), and (d)) gradually blocked off the tail pipe and forced the gas through the cascade. In the fully actuated position, modeling clay was used to seal off the air leakage around the duckbills. For some of these configurations, thrust-modulation data were obtained.

The asymmetrical blade configurations (6 to 15) are shown in figures 3 and 4. Entrance and exit angles of these blades were not equal and, as a result, entrance and exit effective flow areas were not equal.

The reverse thrust and air-flow characteristics of all reversers with 100-percent tail-pipe blockage were first determined over a range of exhaust-nozzle pressure ratios. Surveys of total pressure and flow angle were made at the discharge of typical symmetrical and asymmetrical bladed reversers. The typical symmetrical bladed reverser was evaluated at various duckbill angles between the fully retracted and fully actuated positions to determine the thrust-modulation characteristics. For the asymmetrical configurations, cascade length-to-span ratios, innerbody length, and external-fairing length were all systematically varied in the investigation.

The symbols and the definitions used in this report are defined in the appendix.

RESULTS AND DISCUSSION

Performance of Tail-Pipe-Cascade-Type Model Thrust Reversers Having Symmetrically Shaped Cascade Blades

The maximum reverse-thrust ratio of a full-scale aircraft reverser occurs when the effective area of the reverser is equal to the effective area of the exhaust nozzle, inasmuch as maximum limiting tail-pipe temperature and pressure prevail at these conditions. These two areas were not equal in all the model-reverser tests. Total model-reverser air flow therefore deviated from that obtained with the model exhaust nozzle alone. In order to correct the basic reverse-thrust ratio of the model so as to determine the thrust reversal obtainable with a properly sized full-scale reverser, basic reverse-thrust ratio of the model was divided by model total air flow. This adjusted value is presented in the figures as reverse-thrust ratio.

Thin, single-curvature blades. - The air-flow and reverse-thrust characteristics of the thin, single-curvature blades having cascade solidities of 1.11 and 1.55 (configurations 1 and 2) are presented in figure 5. (Cascade solidity is defined in the appendix along with other terms.) At a pressure ratio of 2.0, the higher-solidity reverser had a reverse-thrust ratio of about 74 percent as compared with about 64 percent for the lower-solidity reverser.

Total-pressure surveys just inside the discharge of the higher-solidity cascade (configuration 2) are shown in figure 6. In general, the total pressure recovered is essentially the same for all but the first two blades in the cascade.

Thick, double-curvature blades. - The reverse-thrust-ratio characteristics of the thick, double-curvature blades also having cascade solidities of 1.55 and 1.11 (configurations 3 and 4) are presented in figure 7.

At a pressure ratio of 2.0, the higher-solidity reverser had a reverse-thrust ratio of about 80 percent as compared with about 70 percent for the lower-solidity reverser.

The performance of the 1.55-solidity reverser (configuration 4) during modulation was also determined. The modulation was achieved by means of a mechanical linkage that gradually opened the cascade and simultaneously blocked the tail pipe. Basic reverse-thrust ratio, air-flow ratio, and reverse-thrust ratio for configuration 4 are presented in figures 8 to 10. Note that the air-flow ratio during modulation was greater than 100 percent but that the reverse-thrust ratio could be varied from -100 (full forward thrust) to 80 percent.

A flow instability was present, however, during the modulation tests. When the duckbills were partly actuated, air, in addition to that passing through the cascade and the exhaust nozzle, was emitted through holes on each side of the reverser as shown by the arrows on the diagram of figure 10. Because of flow separation off one of the duckbills between angles of 15° and 30°, more air was forced through the holes on one side of the reverser than on the other.

Total-pressure and flow-angle surveys taken at the discharge of configuration 4 are shown in figures 11 to 13. Again it can be seen that, in general, the blades at the rear of the cascade are the most effective in providing reverse thrust and that the total pressure recovered is essentially the same for all but the first two blades.

Configuration 4 was also tested to determine its characteristics under a simulated power failure. When the duckbills were held in the fully actuated position and then released, the aerodynamic forces were such that the duckbills fully retracted and restored full forward thrust.

Mach number and flow-angle surveys obtained at two positions perpendicular to thrust-reverser configuration 4 are presented in figures 14 and 15 for exhaust-nozzle pressure ratios of 1.8 and 2.0. It can be seen that, in general, the flow veered away from the reverser at an angle of about 23° with respect to the reverser axis.

In order to eliminate the undesirable side forces resulting from the unsymmetrical air discharge during modulation of configuration 4, the holes downstream of the cascade were blocked off with a ring (see fig. 2(e)). In addition, modeling clay was inserted around the outside edges of the first three blades to more nearly match the shape of the cascade to the shape of the duckbill and thus more nearly simulate the geometry of a typical full-scale production reverser. The modulation performance of this configuration (configuration 5) is presented in figures 16 to 18. Comparing reverser-performance figures 16 to 18 with figures 8 to 10 shows that the basic reverse-thrust ratio at 100-percent

blockage was reduced about 4 percent, the air-flow ratio about 1 percent, and the reverse-thrust ratio about 4 percent as a result of the blockage. Maximum reverse-thrust ratio for configuration 5 was 76 percent at a pressure ratio of 2.0.

Performance of Tail-Pipe-Cascade-Type Model Thrust Reversers Having Asymmetrically Shaped Cascade Blades

With innerbody. - Air-flow and reverse-thrust characteristics obtained with an 18.0-inch long centerbody (configurations 6 to 10) are presented in figure 19. For all five configurations, air-flow ratio was less than 100 percent. At an exhaust-nozzle pressure ratio of 2.0, the maximum reverse-thrust ratio was 85 percent.

A fairing parallel to the reverser axis was installed on the outside of configuration 8 (configuration 9) to more nearly simulate an actual aircraft installation. Comparing configurations 8 and 9 shows that the reverse-thrust ratio increased by about 2 percent because of the presence of the fairing. Also, a cone (see fig. 3(c)) was installed at the end of the innerbody (configuration 10) to determine its effect on reversal performance. Comparing configurations 9 and 10 shows that, at a pressure ratio of 2.0, the reverse-thrust ratio increased by about 2 percent because of the cone.

Total-pressure and flow-angle surveys obtained at the discharge of configuration 8 at various positions parallel to the reverser axis are presented in figures 20 and 21. Again, in general, it can be seen that the blades at the rear of the cascade are the most effective in creating reversed thrust.

Mach number and flow-angle surveys obtained at two positions perpendicular to the reverser axis of configuration 8 are presented in figures 22 and 23. These surveys indicate that the reversed air veered away from the reverser at an angle of about 18° with respect to the reverser axis.

Without innerbody. - The air-flow and reverse-thrust characteristics of thrust-reverser configurations 11, 12, and 13 without an innerbody are presented in figure 24. These configurations also had air-flow ratios less than 100 percent. Comparing figure 24 with figure 19 shows that at an exhaust-nozzle pressure ratio of 2.0, maximum reverse-thrust ratio increased from 85 to 89 percent as a result of removing the centerbody. This difference is probably due to changes in the cascade-inlet flow conditions.

Various innerbody lengths. - The air-flow and reverse-thrust characteristics of thrust-reverser configurations 14 and 15 with various innerbody lengths are presented in figure 25. It can be seen that, in general, the presence of the centerbody lowered the reverse-thrust ratio. For example, at a pressure ratio of 2.0 and a length-to-span ratio of 2.95, the presence of the innerbody lowered the reverse-thrust ratio from 89 to 86 percent.

SUMMARY OF RESULTS

The reverse-thrust performance of several tail-pipe-cascade-type thrust reversers was obtained over a range of exhaust-nozzle pressure ratios from about 1.2 to 2.4. Both symmetrical and asymmetrical cascade blade shapes were investigated.

A thrust-reverser configuration with a thin, symmetrical cascade-blade shape had a maximum reverse-thrust ratio of 74 percent.

A thrust-reverser configuration with a thick, symmetrical, cascade-blade shape had a maximum reverse-thrust ratio of 76 percent of full forward thrust. In addition, the aerodynamic forces were such that in the event of failure of an actuating linkage, normal full forward thrust would be restored. This thrust reverser also had good thrust modulation characteristics. Thrust could be obtained in any amount from 100 percent forward to 76 percent reverse.

A thrust-reverser configuration having an asymmetrical cascade-blade shape, with a centerbody, had a maximum reverse-thrust ratio of about 88 percent of full forward thrust. A similar configuration, but without a centerbody, had a maximum reverse-thrust ratio of about 90 percent of full forward thrust.

Lewis Flight Propulsion Laboratory
National Advisory Committee for Aeronautics
Cleveland, Ohio, June 28, 1955

APPENDIX - SYMBOLS

The following symbols are used in this report:

F_j jet thrust

P_n exhaust-nozzle total pressure

p_0 ambient pressure in test cell

w_a air flow

δ ratio of absolute total pressure at nozzle inlet to absolute pressure at NACA standard sea-level conditions

θ ratio of absolute total temperature at nozzle inlet to absolute temperature at NACA standard sea-level conditions

φ duckbill half-angle, deg

Definitions

The following definitions are used in this report:

Air-flow ratio is $\dfrac{\text{corrected air flow (total test-rig air flow)}}{\text{corrected air flow passed by exhaust nozzle alone (reverser retracted) at same exhaust-nozzle pressure ratio}}$, $\dfrac{(w_a\sqrt{\theta}/\delta)_r}{(w_a\sqrt{\theta}/\delta)_f}$, percent

Cascade solidity, or solidity is $\dfrac{\text{maximum cascade blade chord length}}{\text{cascade blade spacing}}$

Length-to-span ratio is $\dfrac{\text{maximum cascade length}}{\text{maximum cascade span}}$, $\dfrac{L}{S}$

Basic reverse-thrust ratio is $\dfrac{\text{resultant reverse corrected jet thrust}}{\text{forward corrected jet thrust of exhaust nozzle alone (reverser retracted) at same exhaust-nozzle pressure ratio}}$, $\dfrac{(F_j/\delta)_r}{(F_j/\delta)_f}$, percent

Reverse thrust ratio is $\dfrac{\text{basic reverse-thrust ratio}}{\text{air-flow ratio}}$, $\dfrac{(F_j/\delta)/(F_j/\delta)_f}{(w_a\sqrt{\theta}/\delta)_r/(w_a\sqrt{\theta}/\delta)_f}$, percent

Exhaust-nozzle total pressure is the total pressure measured at the entrance to the cascade. Full reversal is obtained with the tail pipe completely blocked downstream of the cascade.

REFERENCES

1. Sutter, Joseph: Reverse Thrust for Jet Transports. Paper presented at meeting SAE, New York (N.Y.), Apr. 12-15, 1954.

2. Steffen, Fred W., McArdle, Jack G., and Coats, James W.: Performance Characteristics of Hemispherical Target-Type Thrust Reversers. NACA RM E55E18, 1955.

TABLE I. - TAIL-PIPE CASCADE REVERSER CONFIGURATIONS

Configuration	Number of blades	Cascade solidity	Types of blade	Length-to-span ratio	Length of innerbody	Cone on innerbody	External fairing	Remarks
1	4	1.11	Symmetrical, thin, single curvature	1.00	No inner-body	No	No	Cascade curved to fit pipe
2	6	1.55	Symmetrical, thin, single curvature	1.00	No inner-body	No	No	Cascade curved to fit pipe
3	4	1.11	Symmetrical, thick, double curvature	1.00	No inner-body	No	No	Cascade curved to fit pipe
4	6	1.55	Symmetrical, thick, double curvature	1.00	No inner-body	No	No	Cascade curved to fit pipe
5	6	1.55	Symmetrical, thick, double curvature	1.00	No inner-body	No	No	Cascade curved to fit pipe plus external blockage
6	14	1.625	Asymmetrical, thin, single curvature	2.95	18.00	No	No	Flat cascade
7	10	1.625	Asymmetrical, thin, single curvature	1.27	18.00	No	No	Flat cascade
8	7	1.625	Asymmetrical, thin, single curvature	2.14	18.00	No	No	Cascade curved to fit pipe
9	7	1.625	Asymmetrical, thin, single curvature	2.14	18.00	No	Yes	Cascade curved to fit pipe
10	7	1.625	Asymmetrical, thin, single curvature	2.14	19.75	Yes	Yes	Cascade curved to fit pipe
11	14	1.625	Asymmetrical, thin, single curvature	2.95	No inner-body	No	No	Flat cascade
12	10	1.625	Asymmetrical, thin, single curvature	1.27	No inner-body	No	No	Flat cascade
13	7	1.625	Asymmetrical, thin, single curvature	0.56	No inner-body	No	Yes	Cascade curved to fit pipe
14(a)	14	1.625	Asymmetrical, thin, single curvature	2.95	No inner-body	No	No	Flat cascade
14(b)	14	1.625	Asymmetrical, thin, single curvature	2.95	18.00	No	No	Flat cascade
15(a)	10	1.625	Asymmetrical, thin, single curvature	1.27	No inner-body	No	No	Flat cascade
15(b)	10	1.625	Asymmetrical, thin, single curvature	1.27	10.15	No	No	Flat cascade
15(c)	10	1.625	Asymmetrical, thin, single curvature	1.27	11.90	No	No	Flat cascade
15(d)	10	1.625	Asymmetrical, thin, single curvature	1.27	13.15	No	No	Flat cascade
15(e)	10	1.625	Asymmetrical, thin, single curvature	1.27	18.00	No	No	Flat cascade

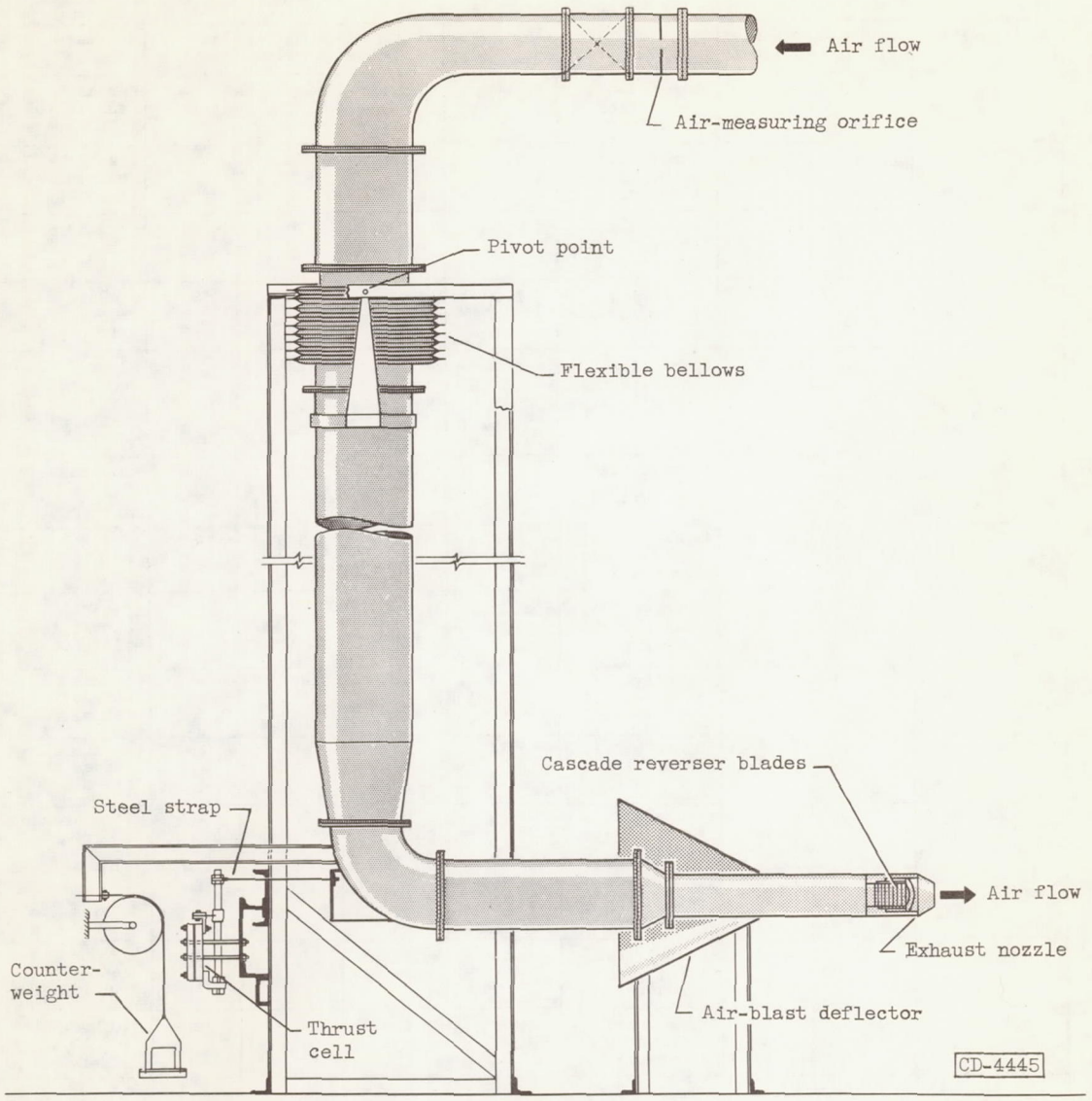

Figure 1. - Schematic diagram of setup for thrust-reversal investigation.

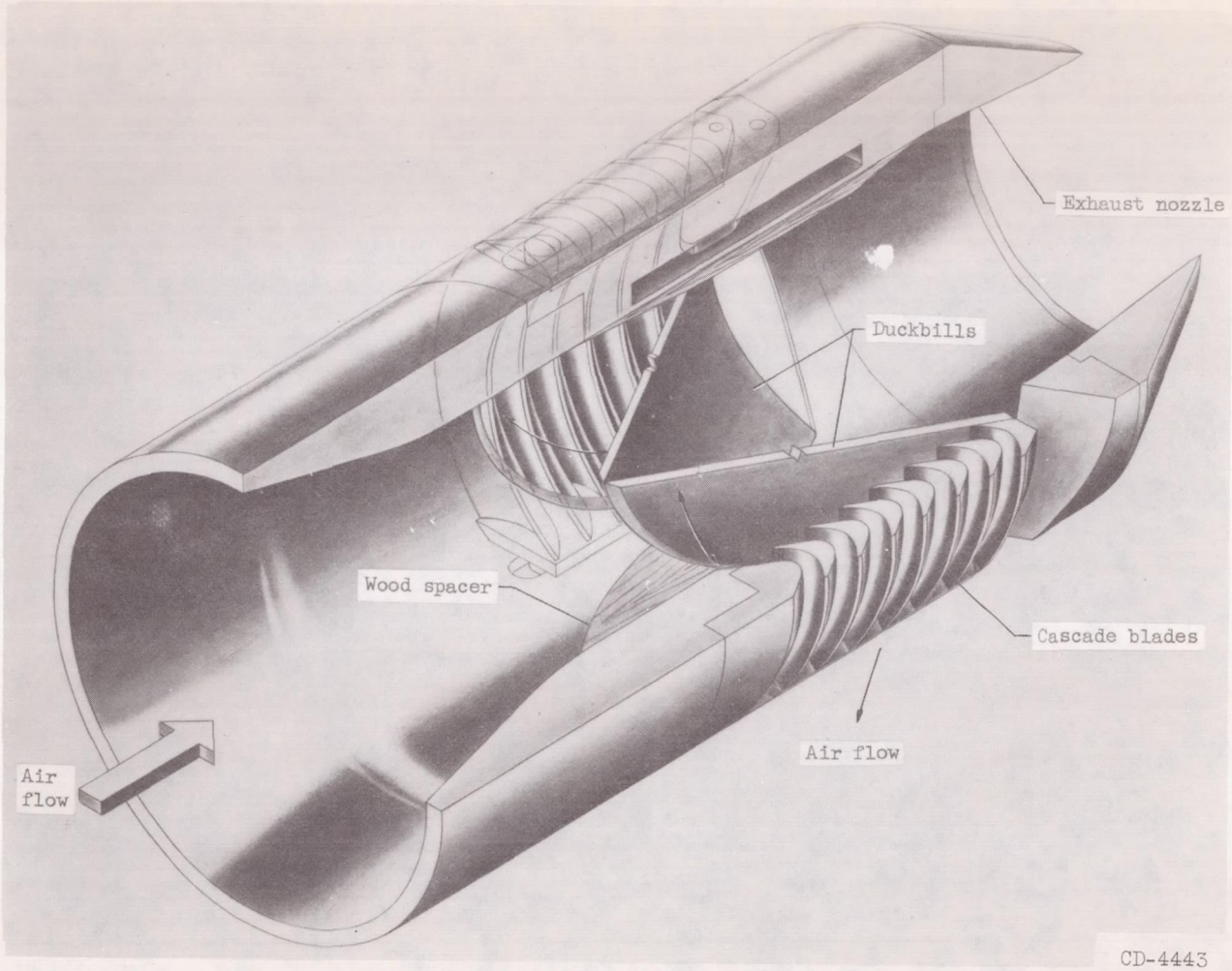

(a) One-quarter cutaway isometric drawing. Fully actuated position.

Figure 2. - Tail-pipe-cascade-type thrust reverser having symmetrical cascade blades (typical of configurations 1 to 5).

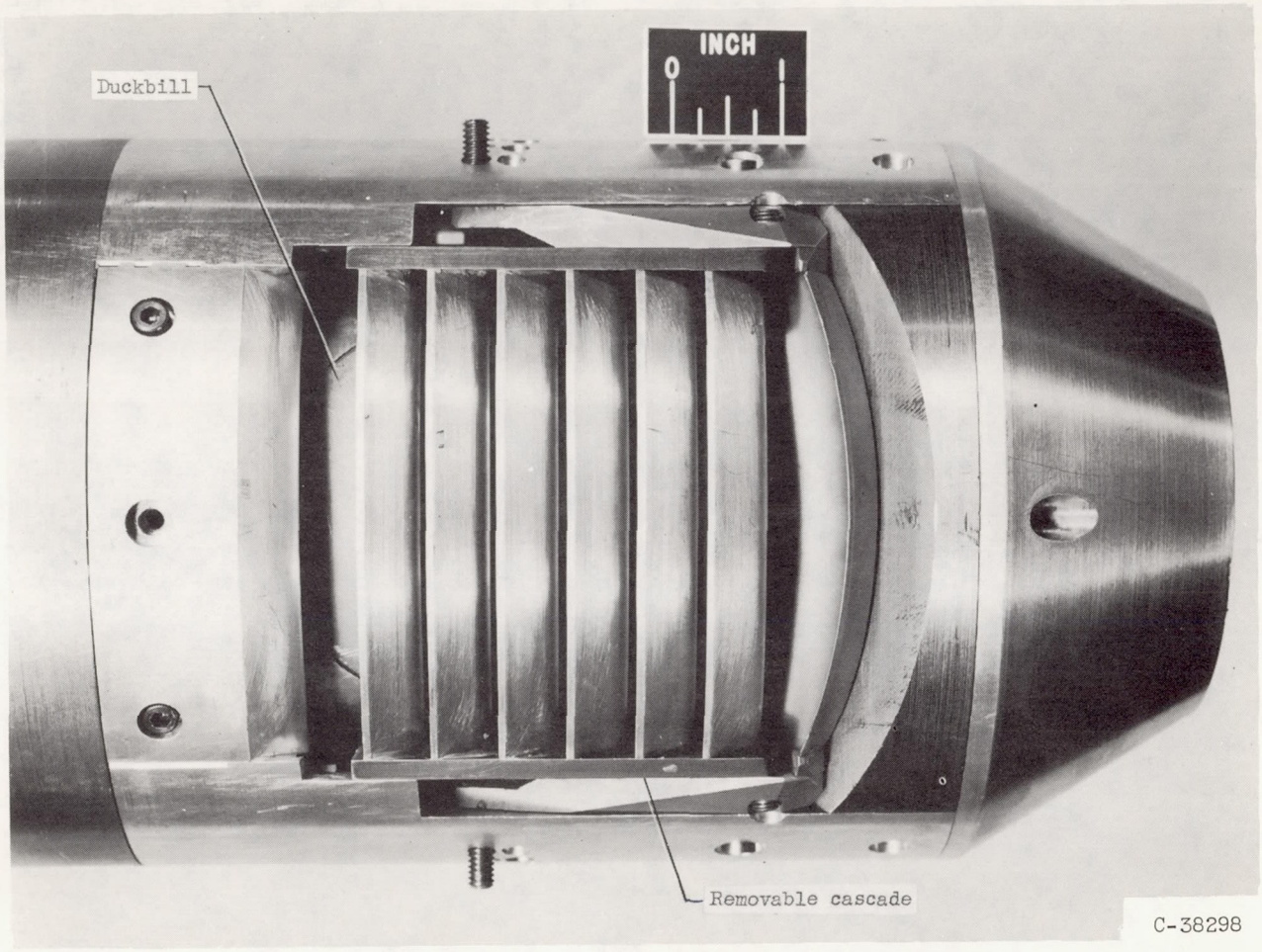

(b) Side view. Fully retracted position.

Figure 2. - Continued. Tail-pipe-cascade-type thrust reverser having symmetrical cascade blades (typical of configurations 1 to 5).

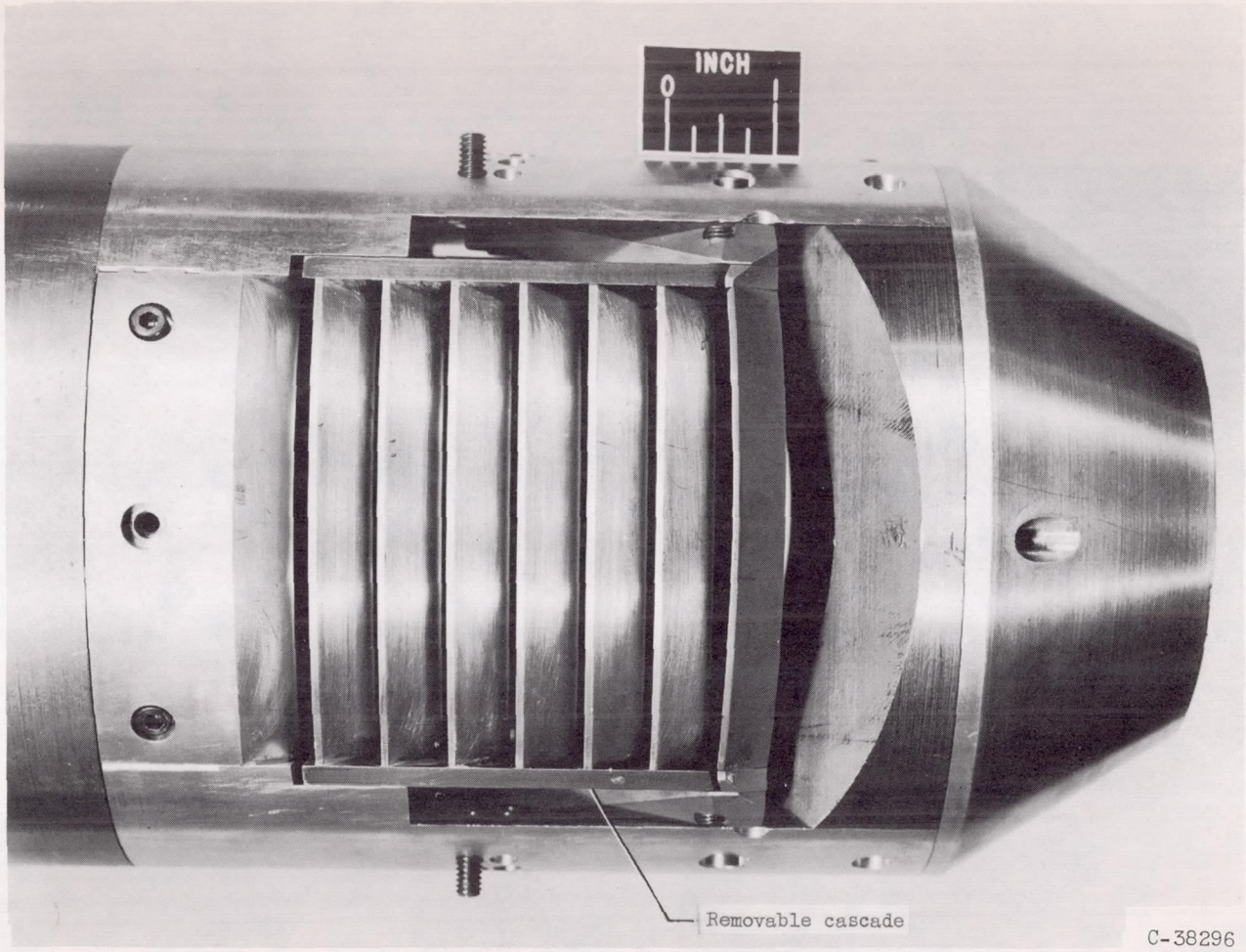

(c) Side view. Fully actuated position.

Figure 2. - Continued. Tail-pipe-cascade-type thrust reverser having symmetrical cascade blades (typical of configurations 1 to 5).

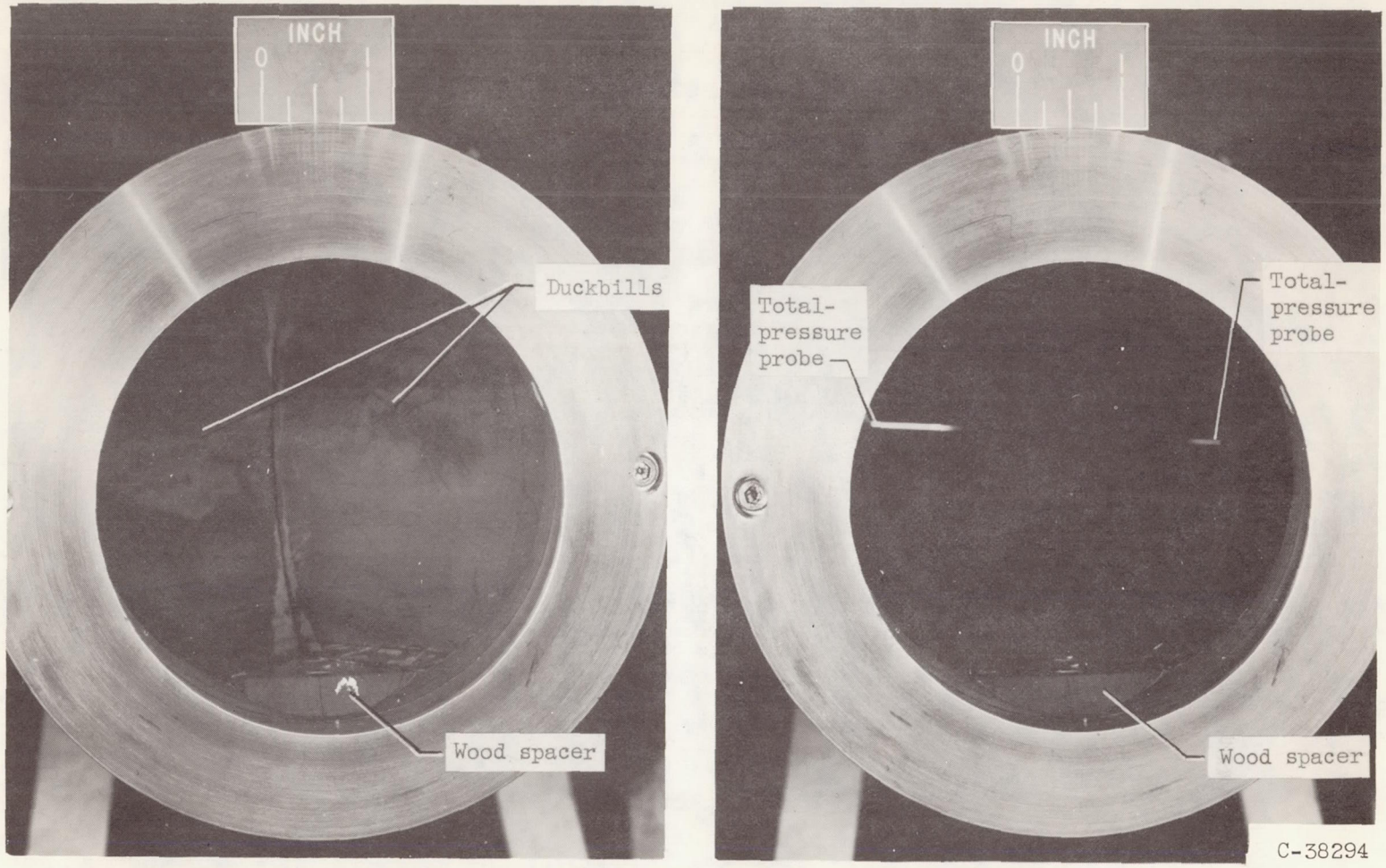

Fully actuated

Fully retracted

(d) View looking upstream.

Figure 2. - Continued. Tail-pipe-cascade-type thrust reverser having symmetrical cascade blades (typical of configurations 1 to 5).

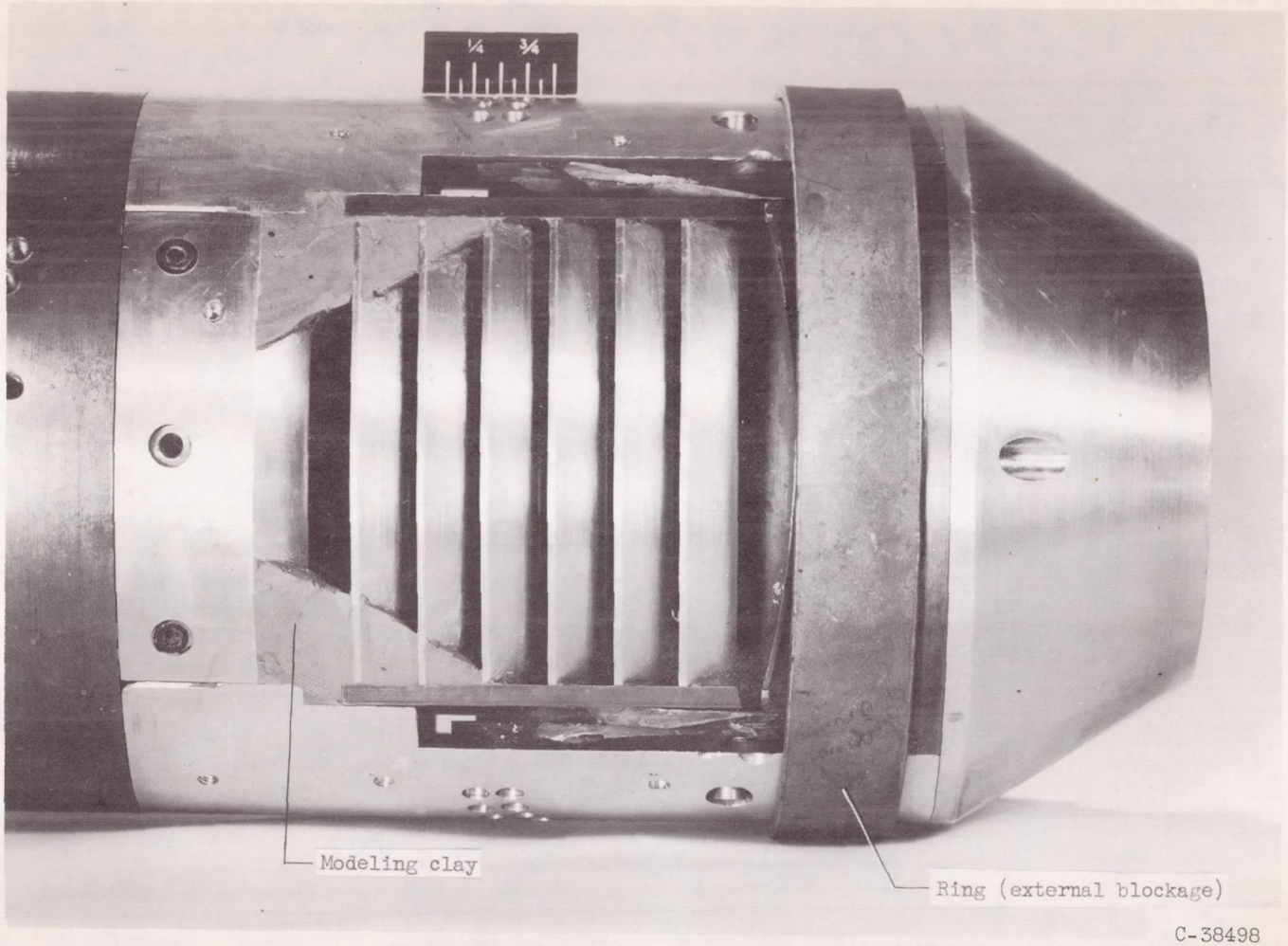

C-38498

(e) Side view of configuration 5 (model thrust reverser most nearly simulating a typical full-scale-aircraft thrust reverser.)

Figure 2. - Continued. Tail-pipe-cascade-type thrust reverser having symmetrical cascade blades (typical of configurations 1 to 5).

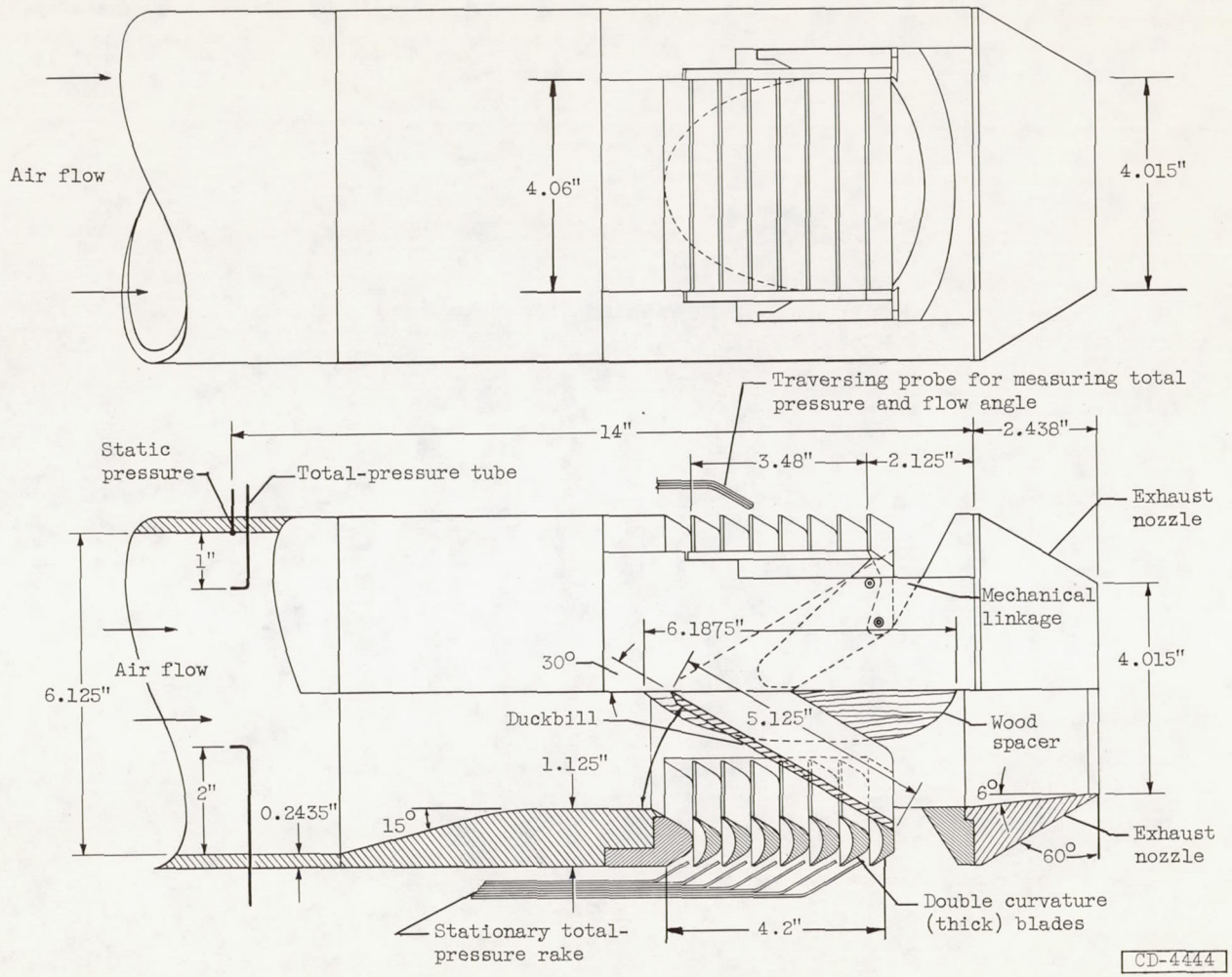

(f) Typical instrumentation.

Figure 2. - Continued. Tail-pipe-cascade-type thrust reverser having symmetrical cascade blades (typical of configurations 1 to 5).

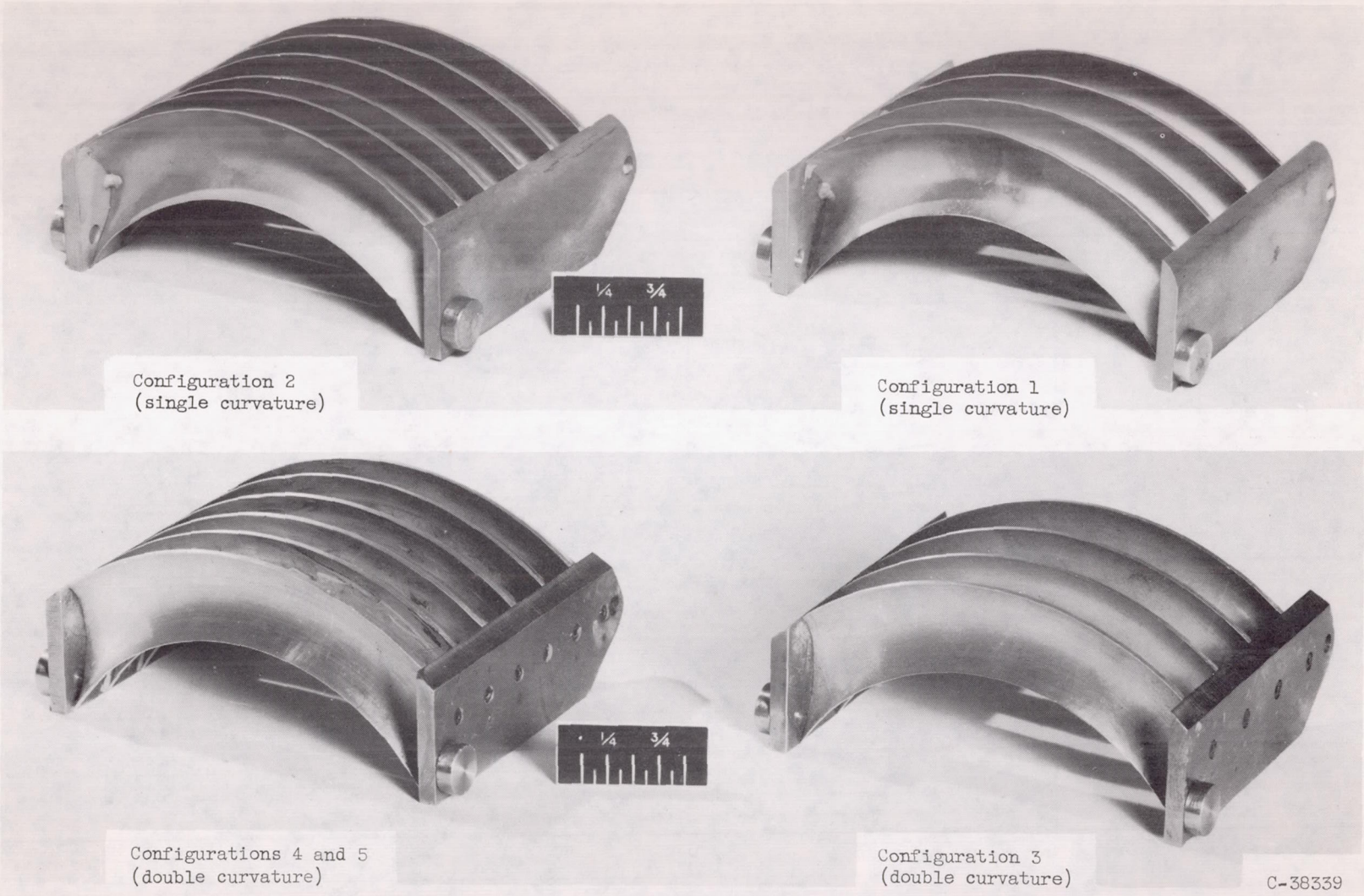

(g) Photograph of blades used in various configurations.

Figure 2. - Continued. Tail-pipe-cascade-type thrust reverser having symmetrical cascade blades (typical of configurations 1 to 5).

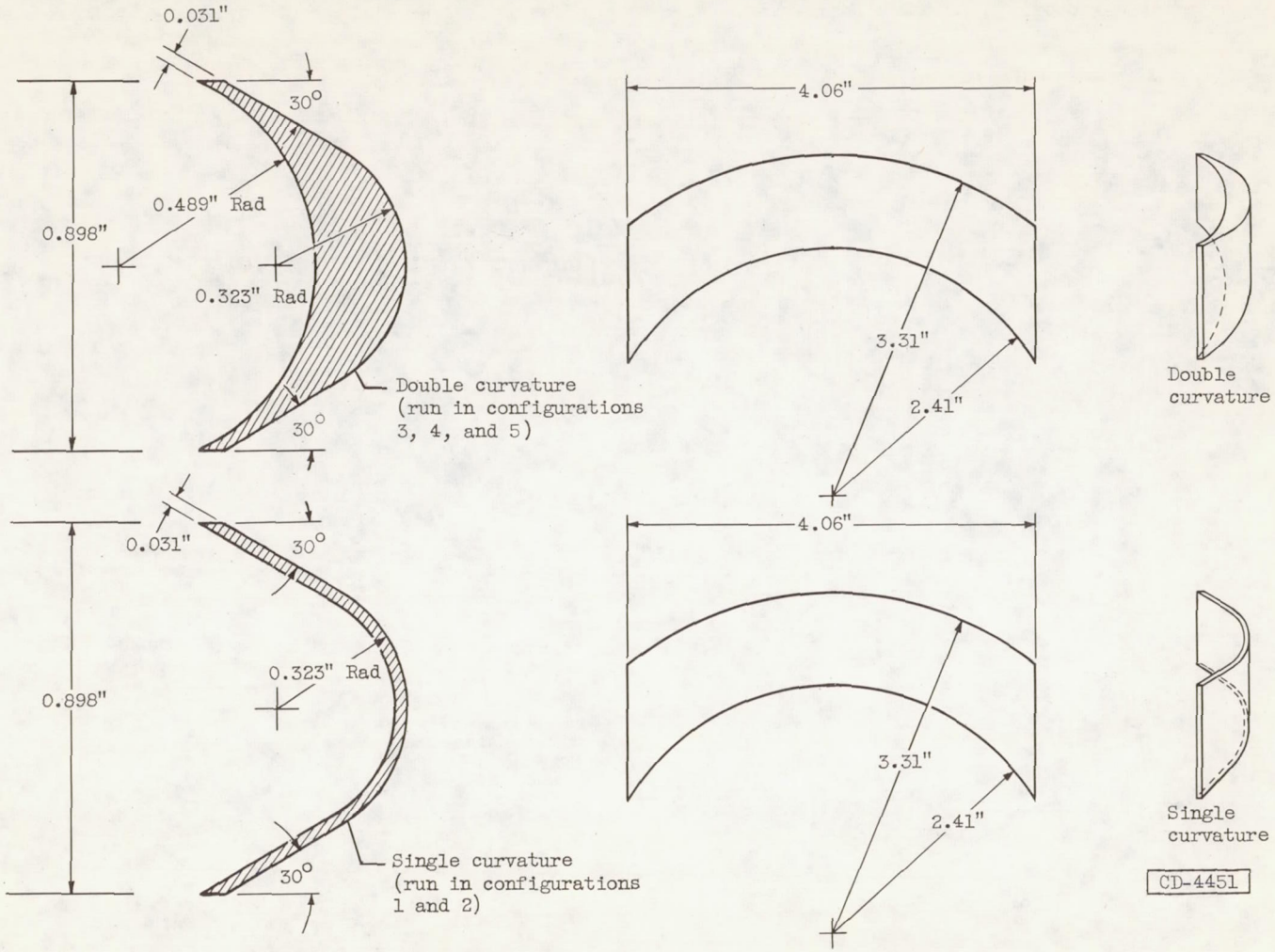

(h) Schematic diagram of blades used in various configurations.

Figure 2. - Concluded. Tail-pipe-cascade-type thrust reverser having symmetrical cascade blades (typical of configurations 1 to 5).

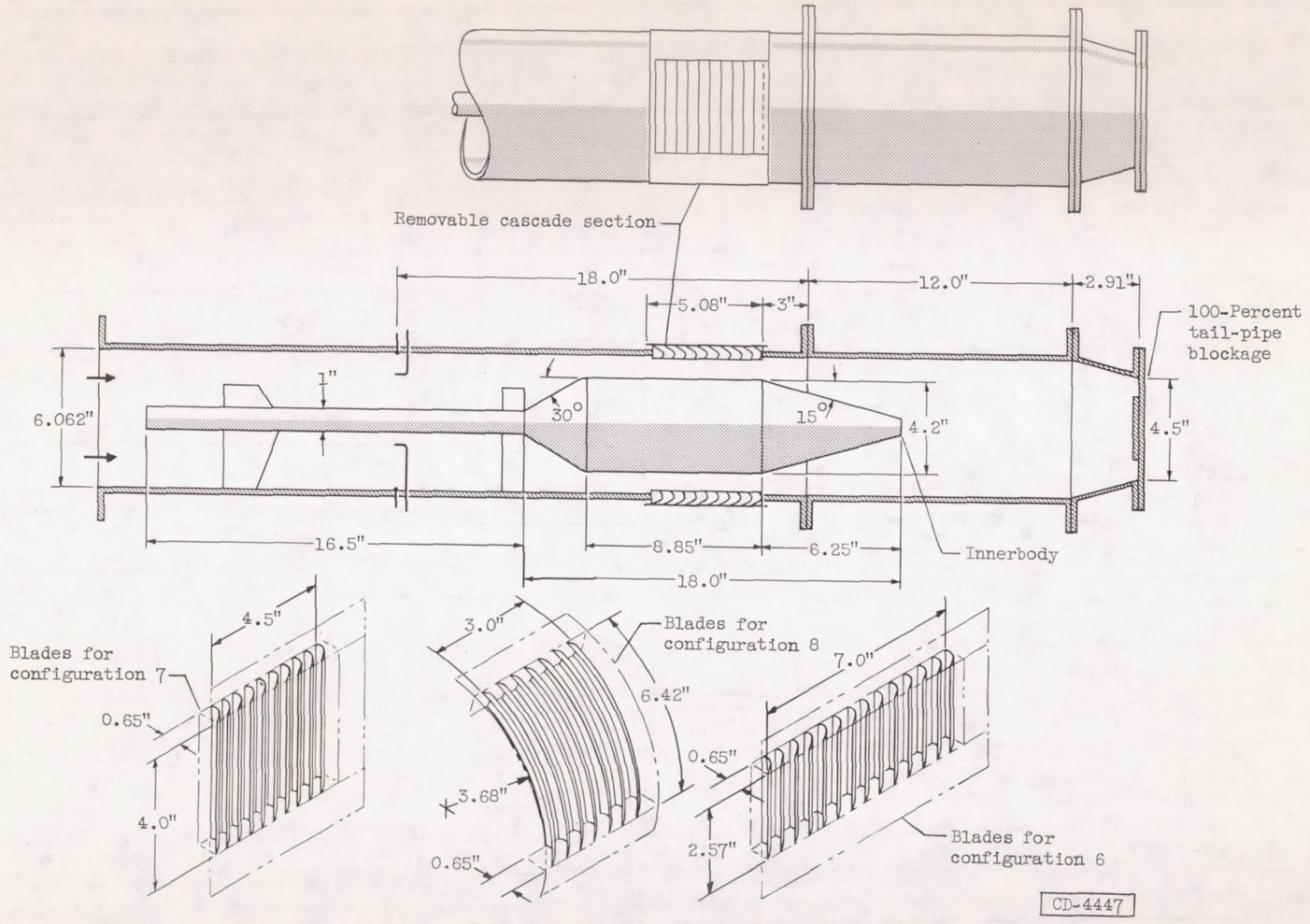

(a) Configurations 6, 7, and 8.

Figure 3. - Schematic diagram of tail-pipe-cascade-type thrust reverser having asymmetrical cascade blade shapes. (Configurations 6 to 15.)

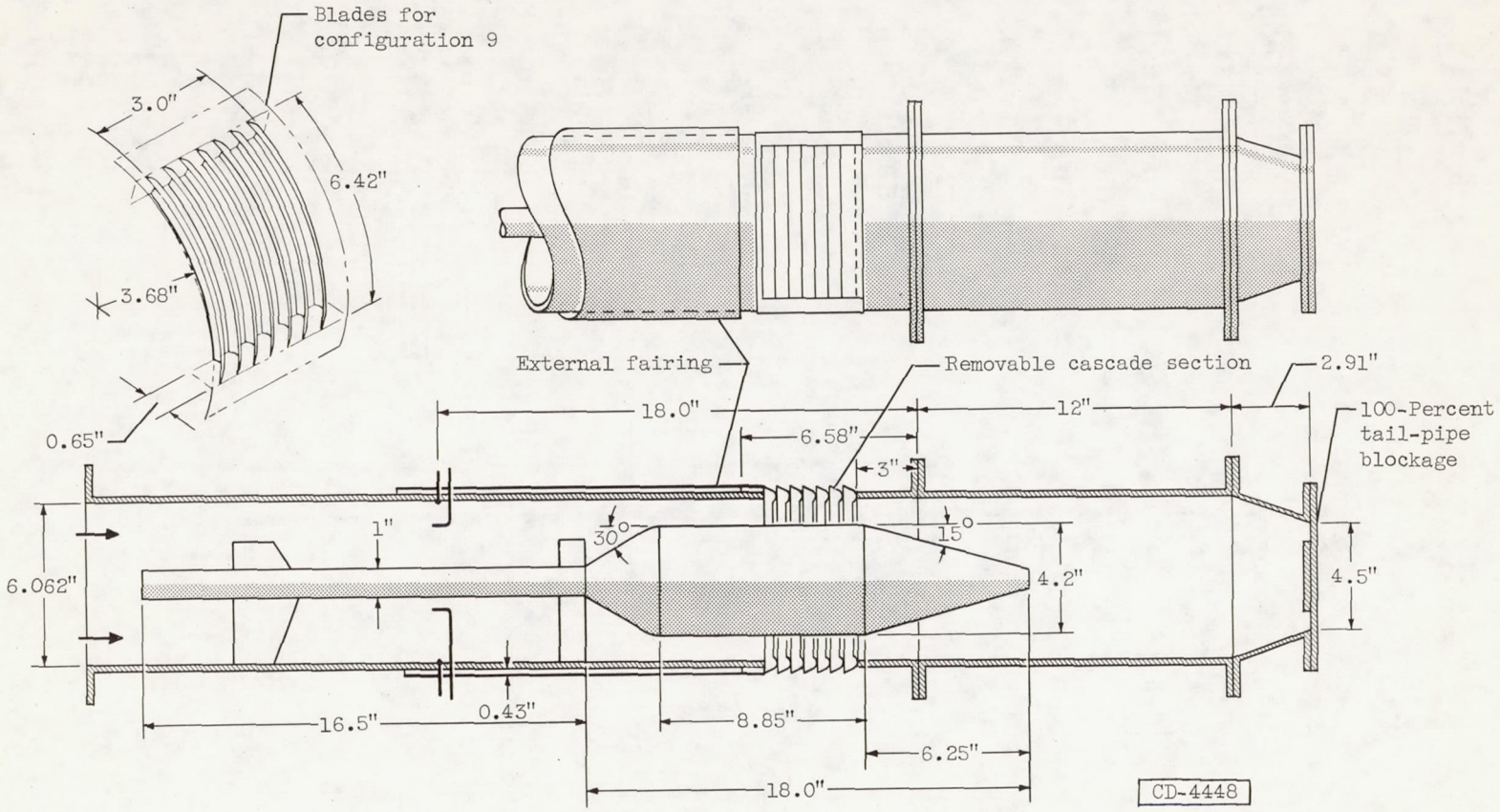

(b) Configuration 9.

Figure 3. - Continued. Schematic diagram of tail-pipe-cascade-type thrust reverser having asymmetrical cascade blade shapes. (Configurations 6 to 15.)

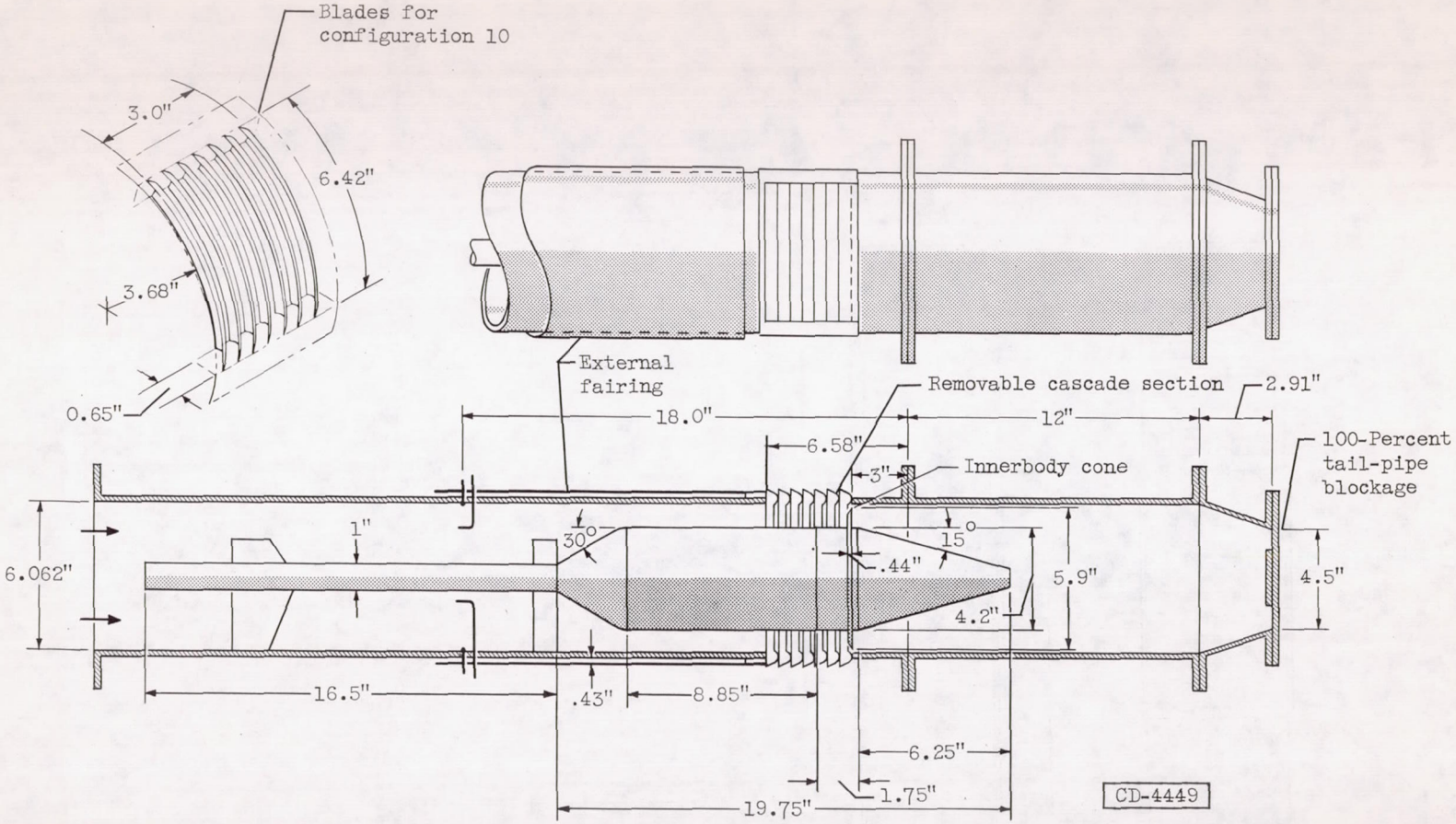

(c) Configuration 10.

Figure 3. - Continued. Schematic diagram of tail-pipe-cascade-type thrust reverser having asymmetrical cascade blade shapes. (Configurations 6 to 15.)

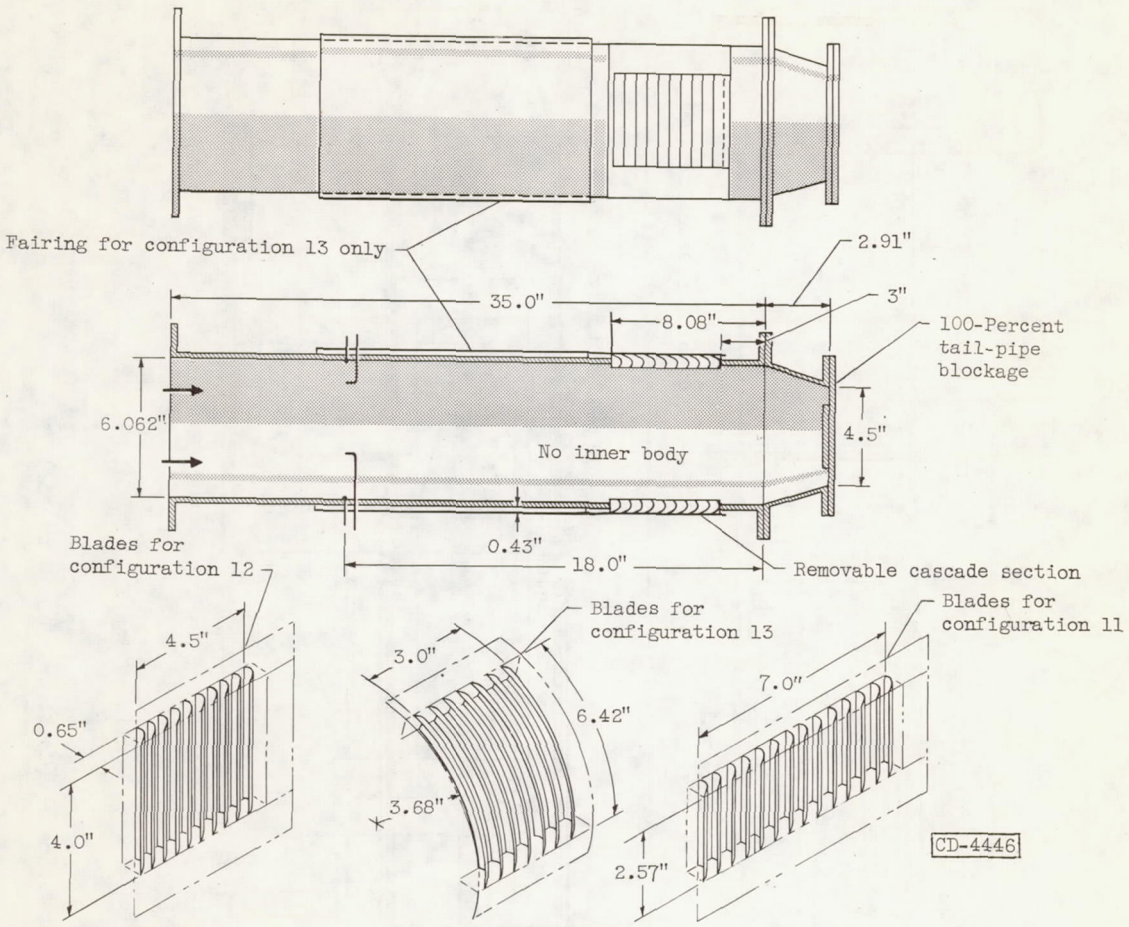

(d) Configurations 11, 12, and 13.

Figure 3. - Continued. Schematic diagram of tail-pipe-cascade-type thrust reverser having asymmetrical cascade blade shapes. (Configurations 6 to 15.)

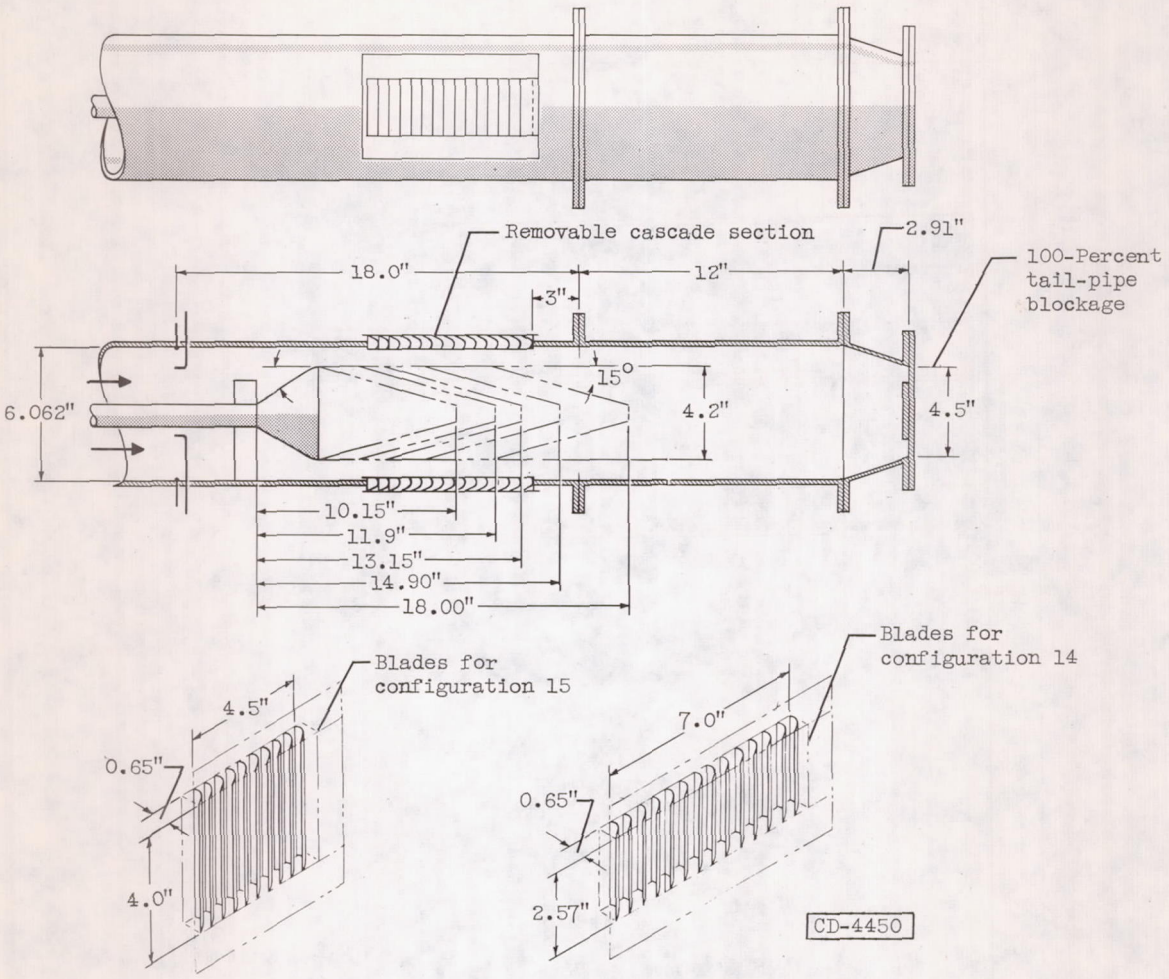

(e) Configurations 14 and 15.

Figure 3. - Concluded. Schematic diagram of tail-pipe-cascade-type thrust reverser having asymmetrical cascade blade shapes. (Configuration 6 to 15.)

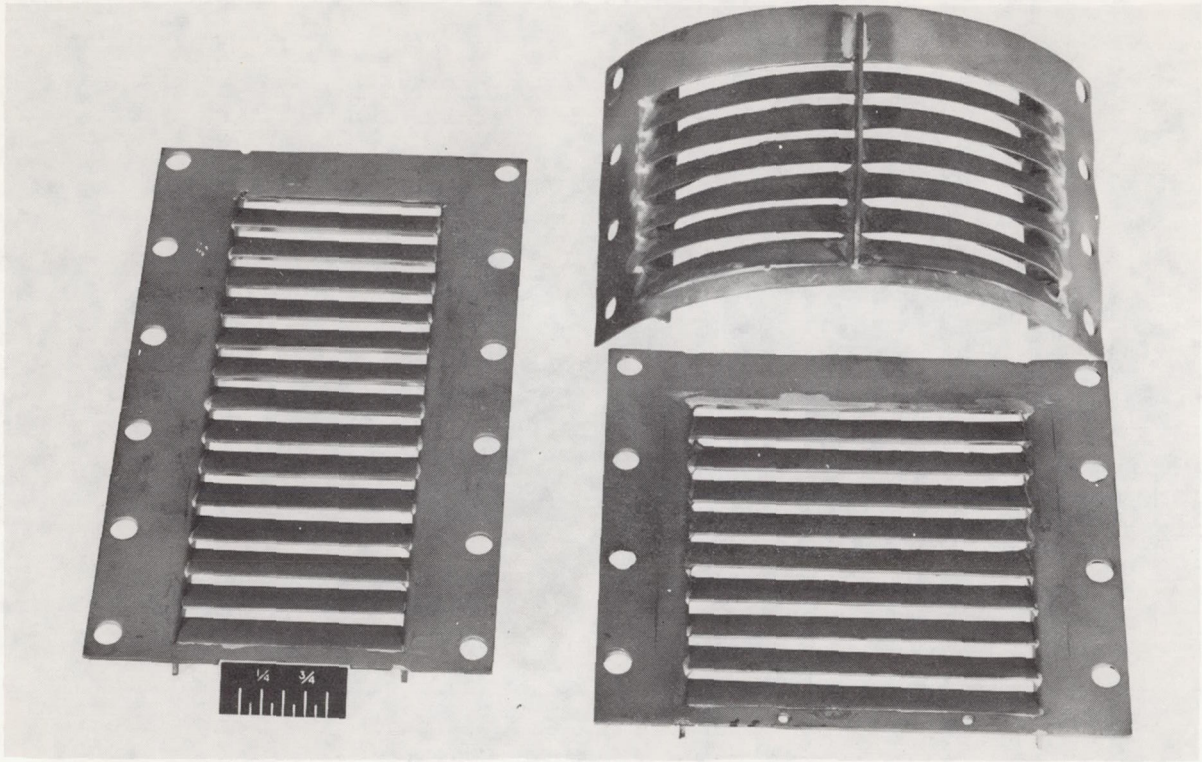

(a) Configurations 6 to 15.

Figure 4. - Asymmetrical cascade blades used in model thrust reversers 6 to 15.

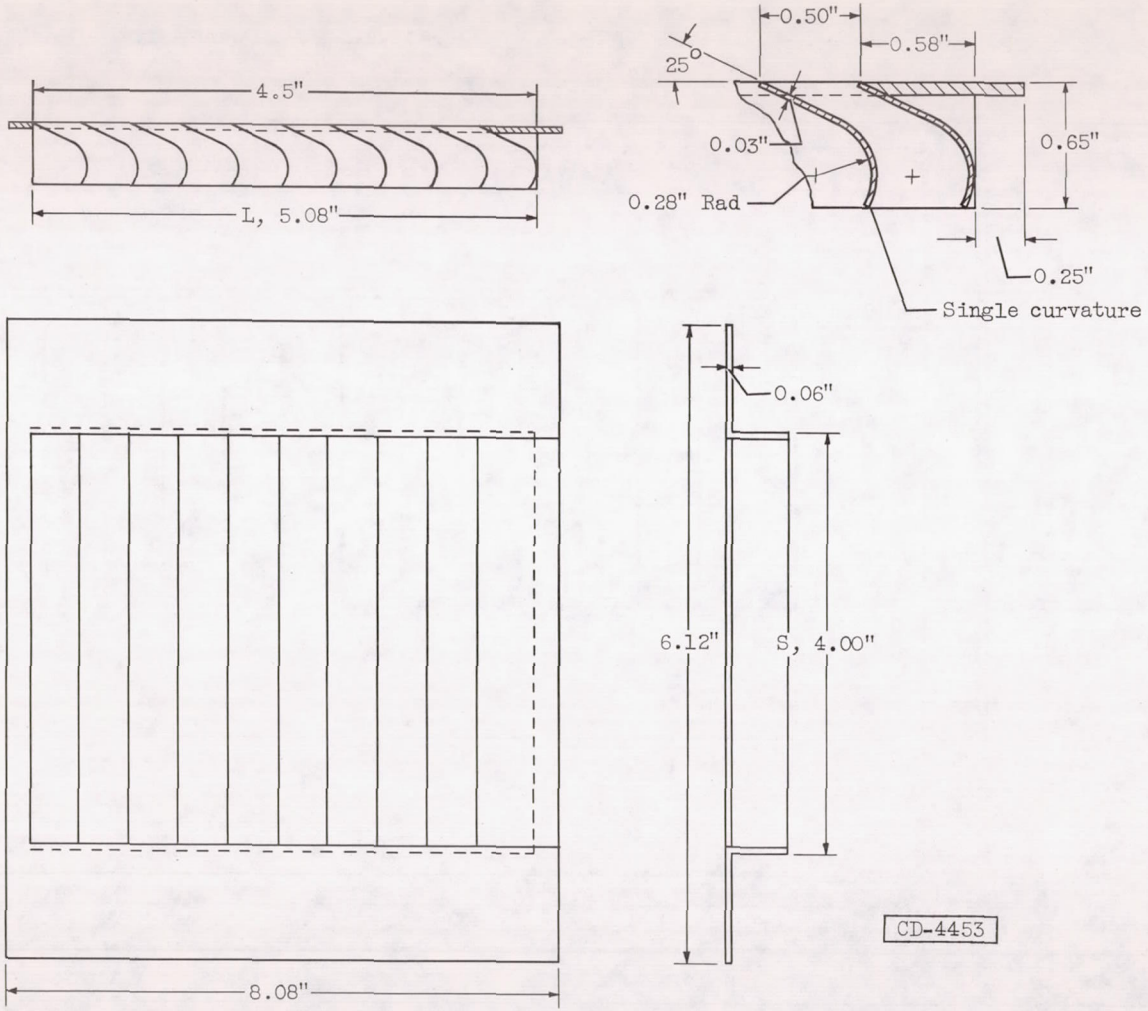

(b) Configurations 6, 11, and 15. Length-span ratio, 1.27.

Figure 4. - Continued. Asymmetrical cascade blades used in model thrust reversers 6 to 15.

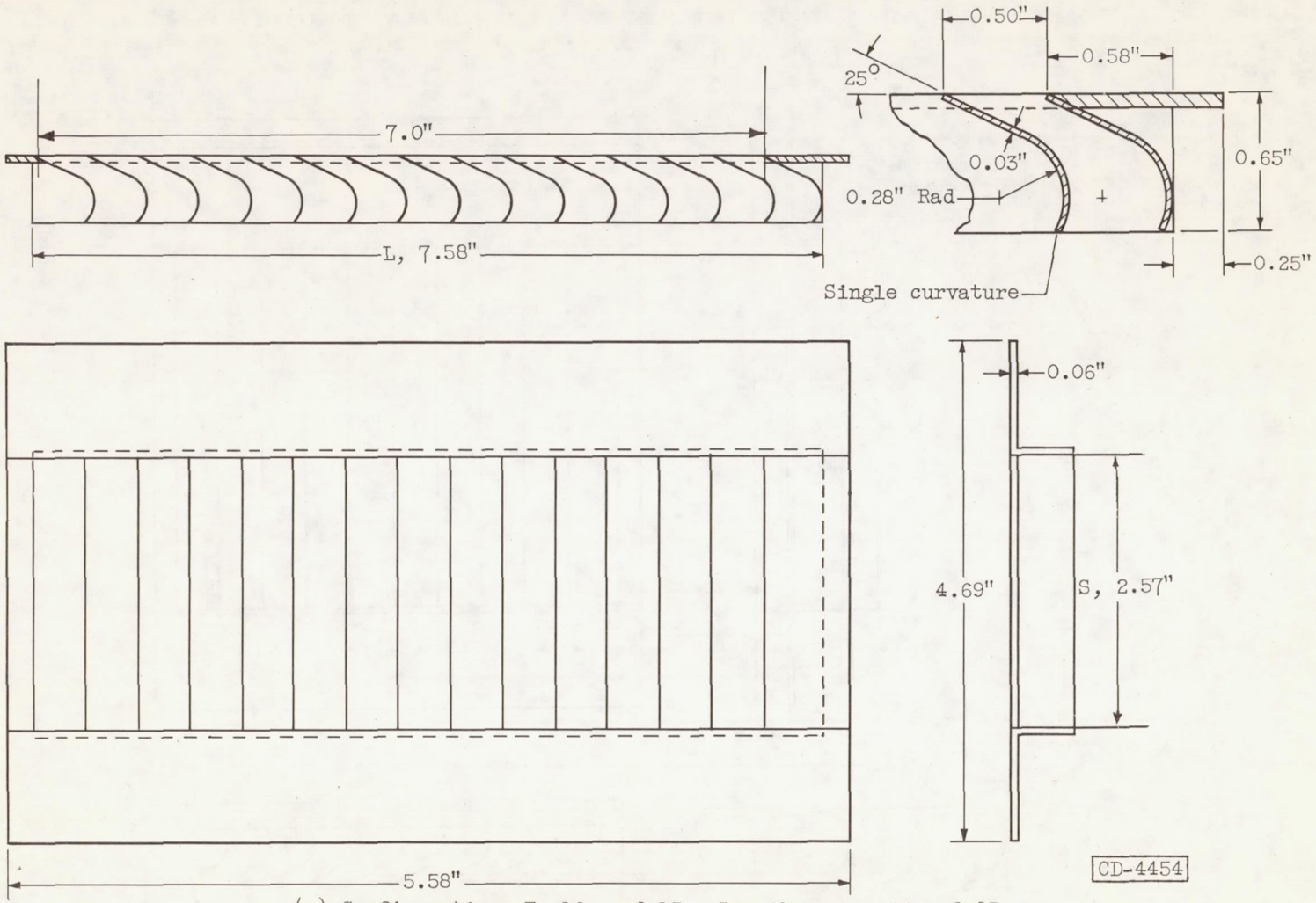

(c) Configurations 7, 12, and 15. Length-span ratio, 2.95.

Figure 4. - Continued. Asymmetrical cascade blades used in model thrust reversers 6 to 15.

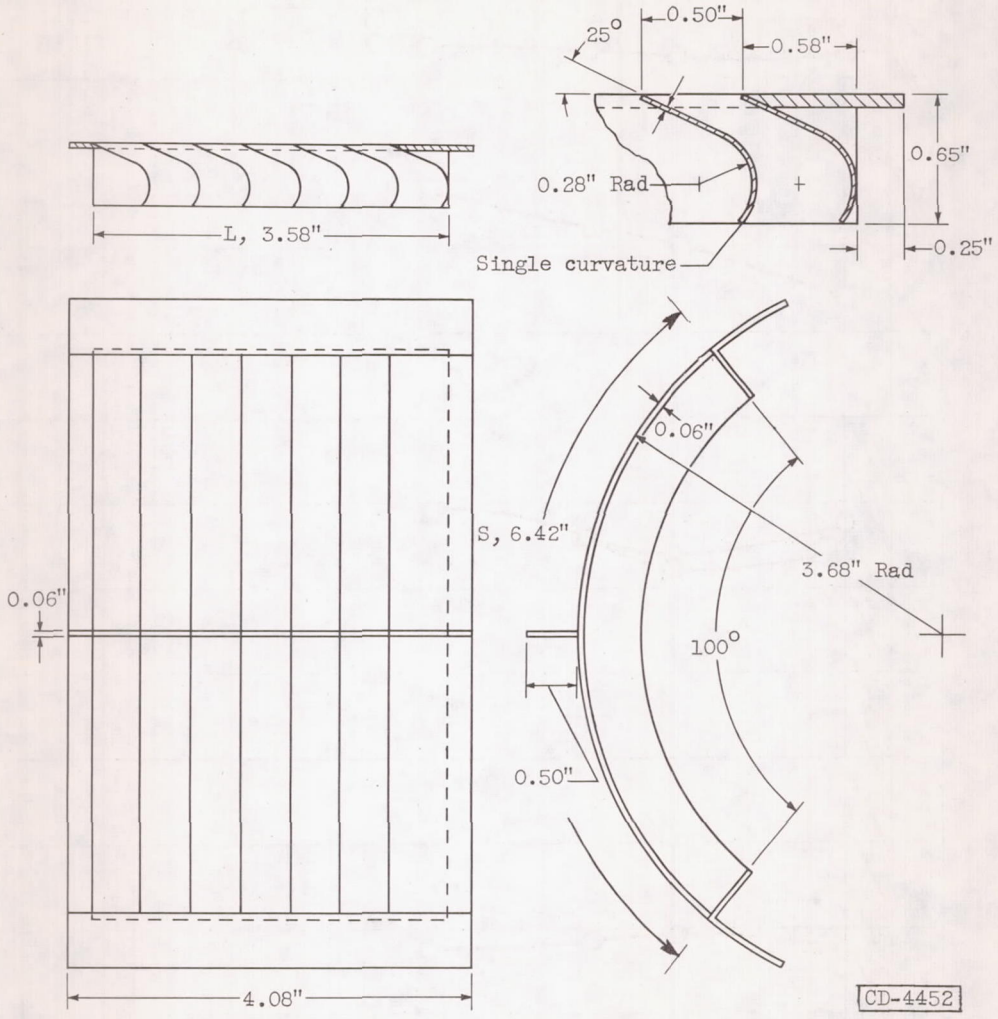

(d) Configurations 8, 9, 10, and 13. Length-span ratio, 0.56.

Figure 4. - Concluded. Asymmetrical cascade blades used in model thrust reversers 6 to 15.

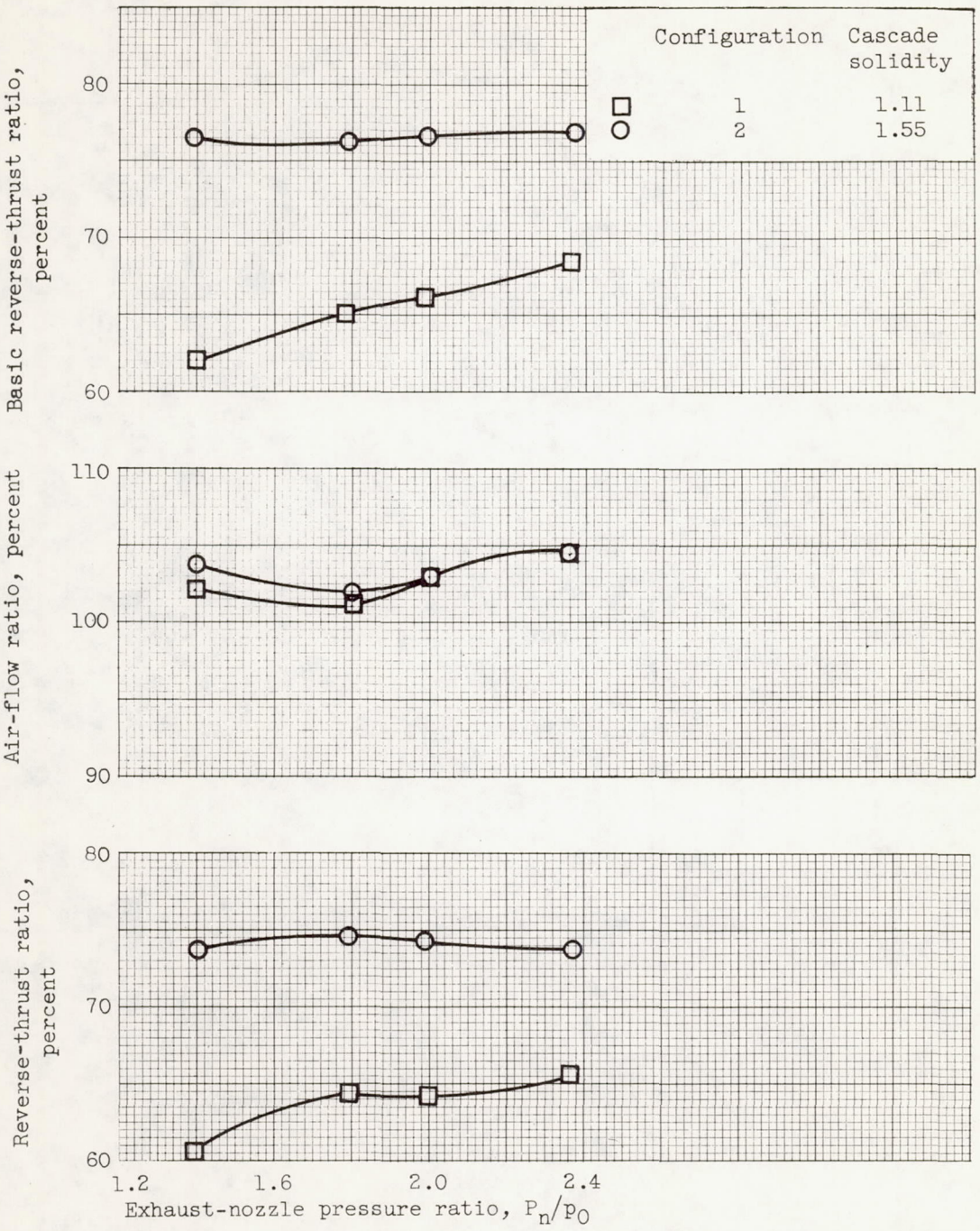

Figure 5. - Air-flow and thrust-reversal characteristics of two tailpipe-cascade-type thrust reversers over range of exhaust-nozzle pressure ratios; full reversal; symmetrical, single-curvature blades.

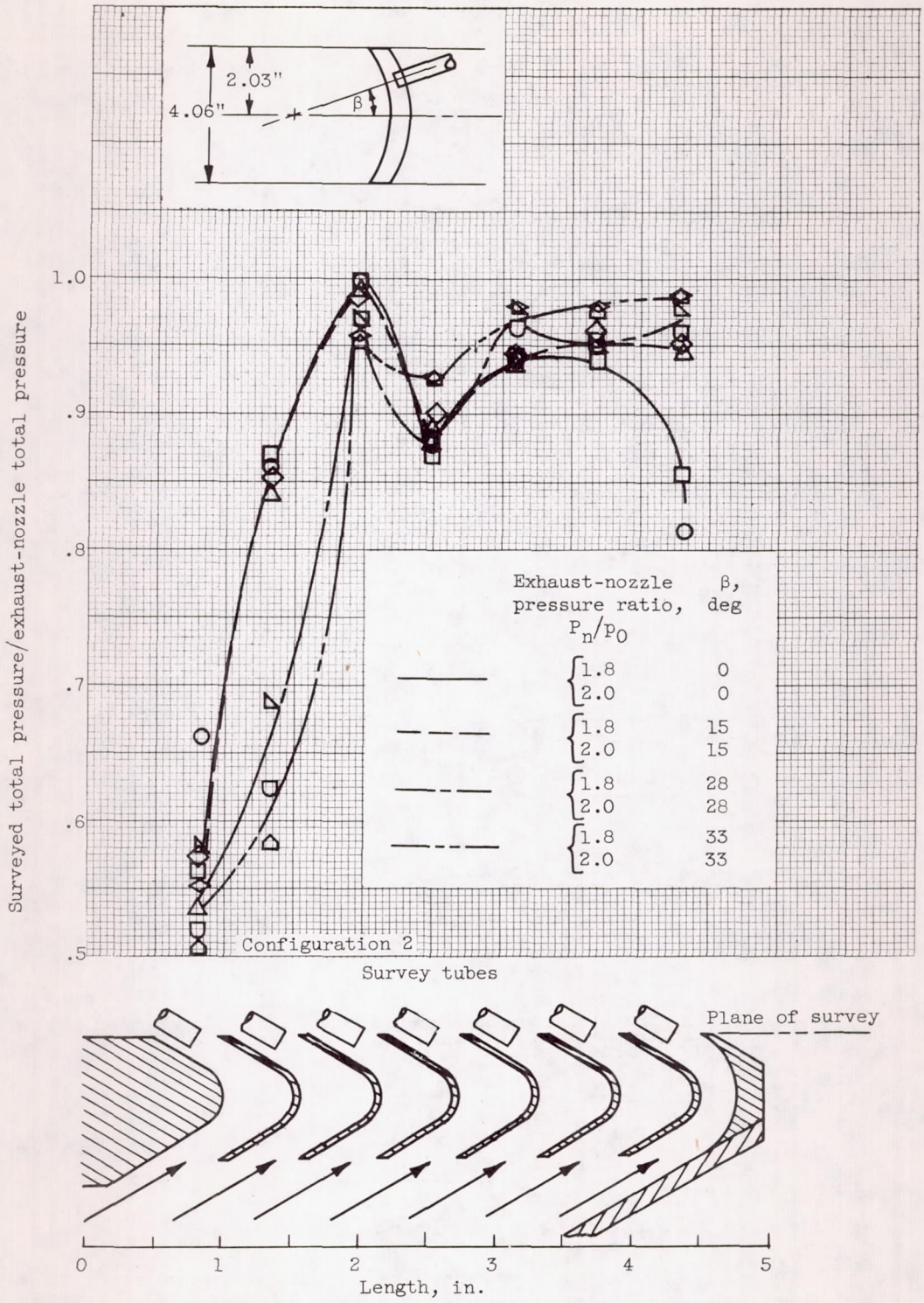

Figure 6. - Total-pressure surveys at the discharge of tail-pipe-cascade-type thrust reverser. Cascade solidity, 1.55; symmetrical, single-curvature blades; full reversal.

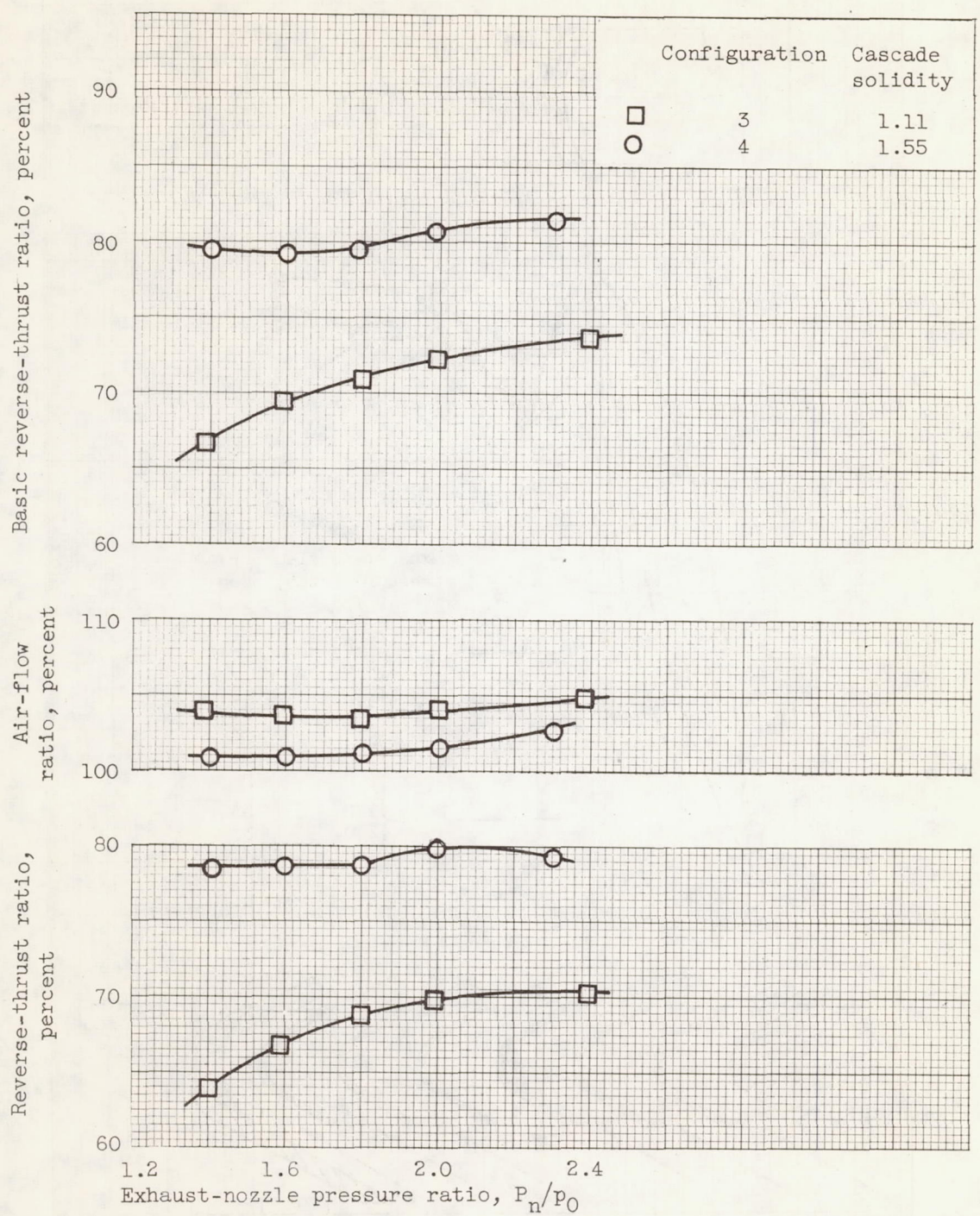

Figure 7. - Air-flow and thrust-reversal characteristics of two tail-pipe-cascade-type thrust reversers over range of exhaust-nozzle pressure ratios; full reversal; symmetrical, double-curvature blades.

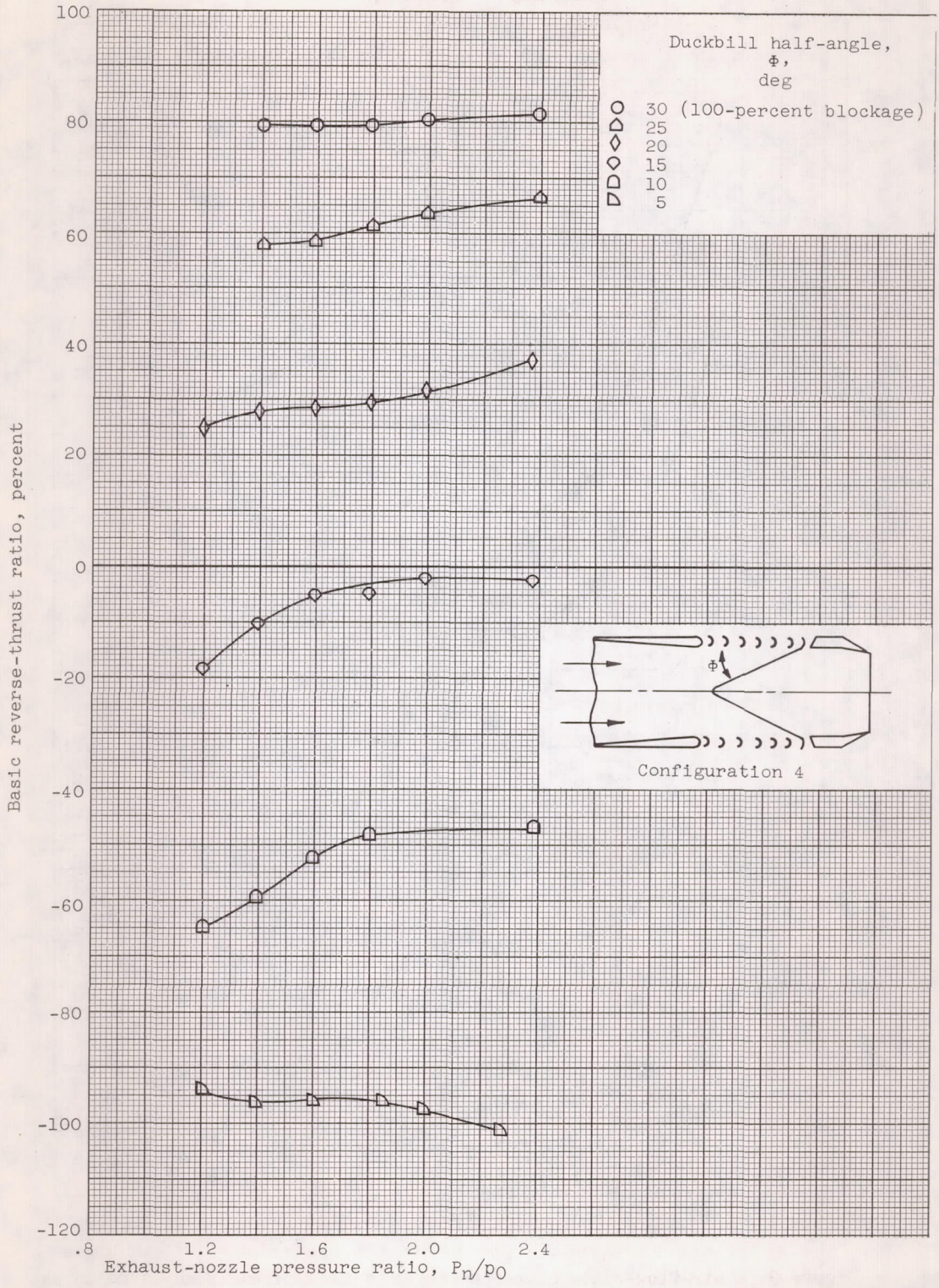

Figure 8. - Thrust-reversal characteristics of tail-pipe-cascade-type thrust reverser at various duckbill half-angles over a range of exhaust-nozzle pressure ratios. Cascade solidity, 1.55; symmetrical, double-curvature blades.

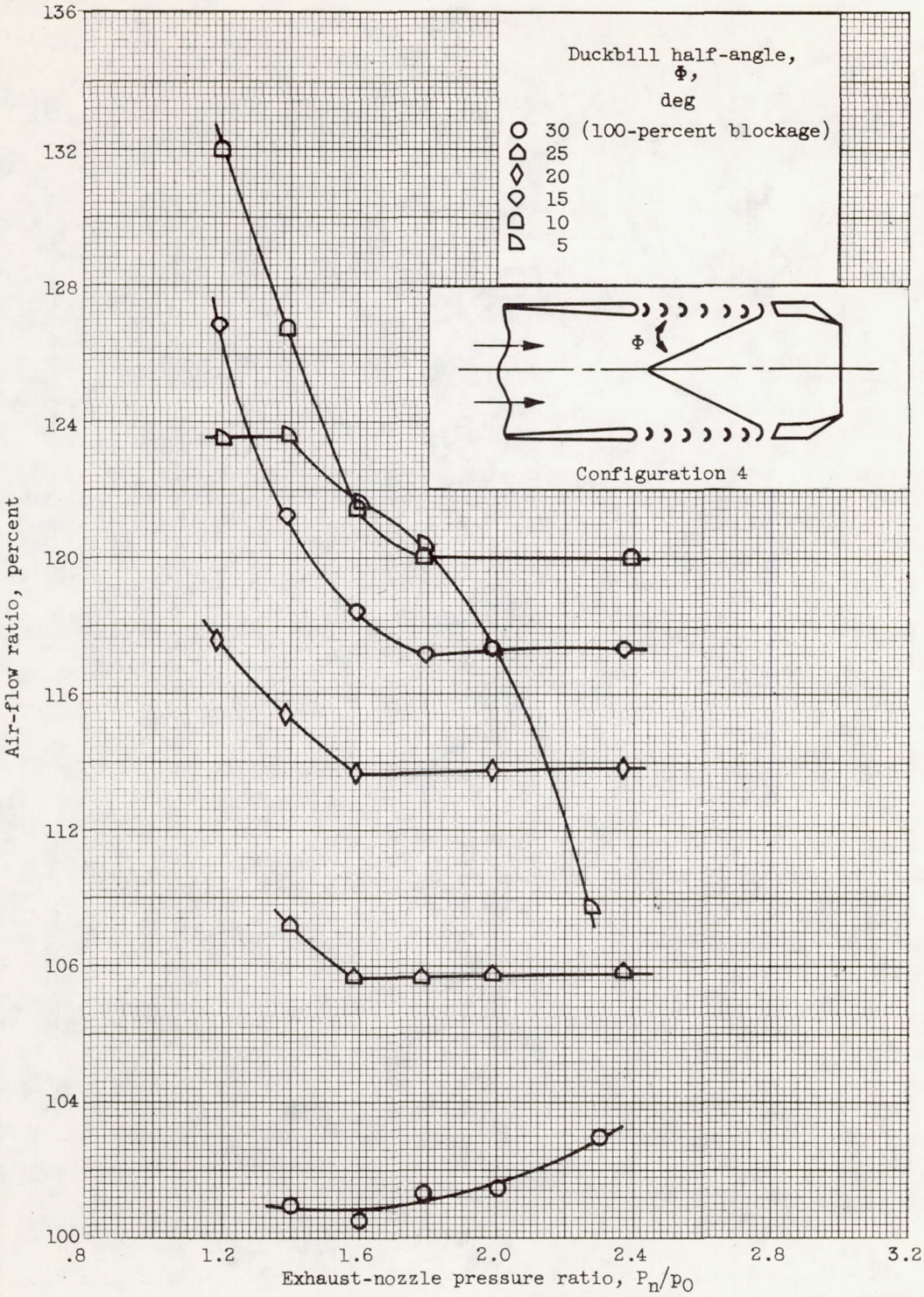

Figure 9. - Air-flow-ratio characteristics of tail-pipe-cascade-type thrust reverser at various duckbill half-angles over a range of exhaust-nozzle pressure ratios. Cascade solidity, 1.55; symmetrical, double-curvature blades.

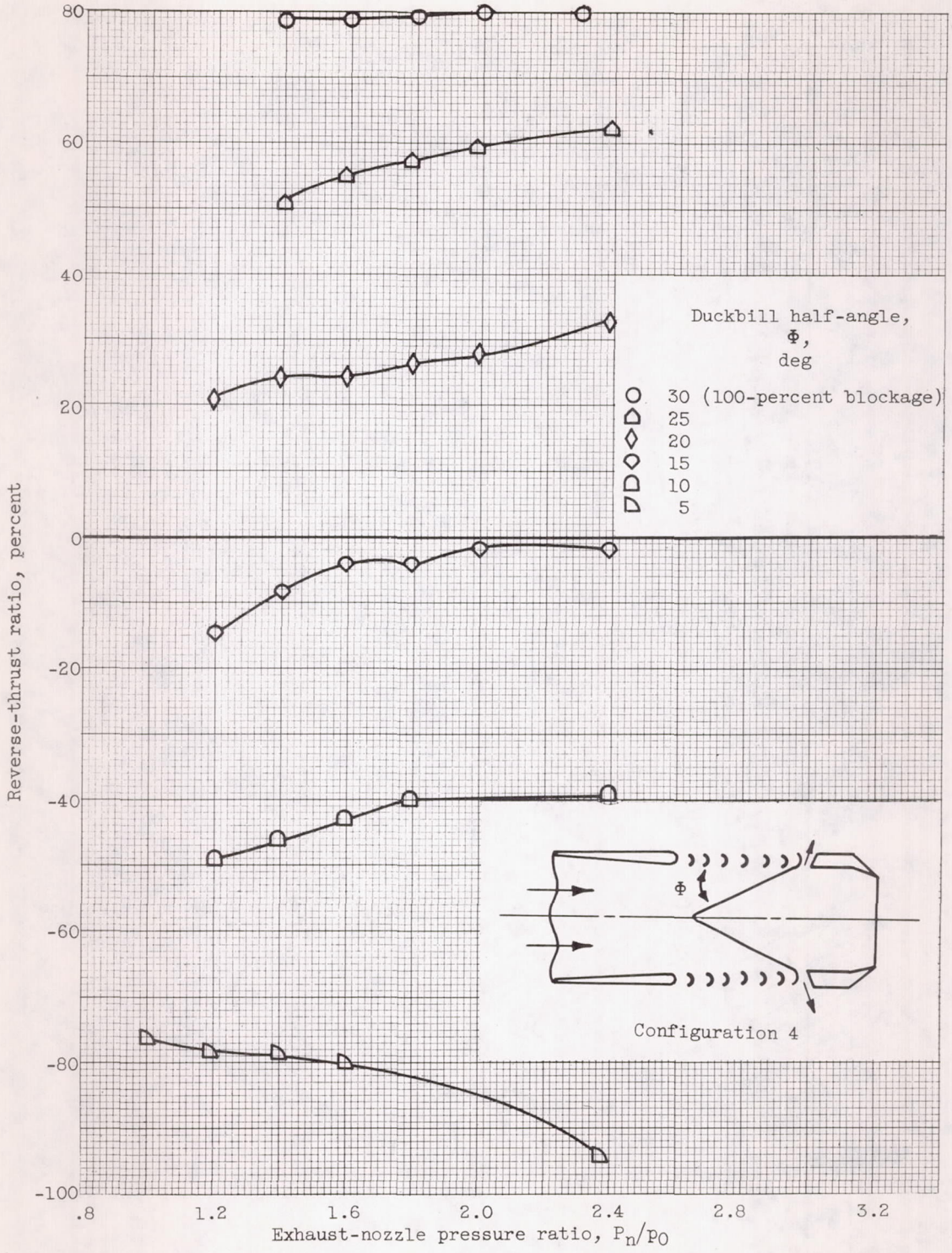

Figure 10. - Reverse-thrust ratio characteristics of tail-pipe-cascade type thrust reverser at various duckbill half-angles over a range of exhaust-nozzle pressure ratios. Cascade solidity, 1.55; symmetrical, double-curvature blades.

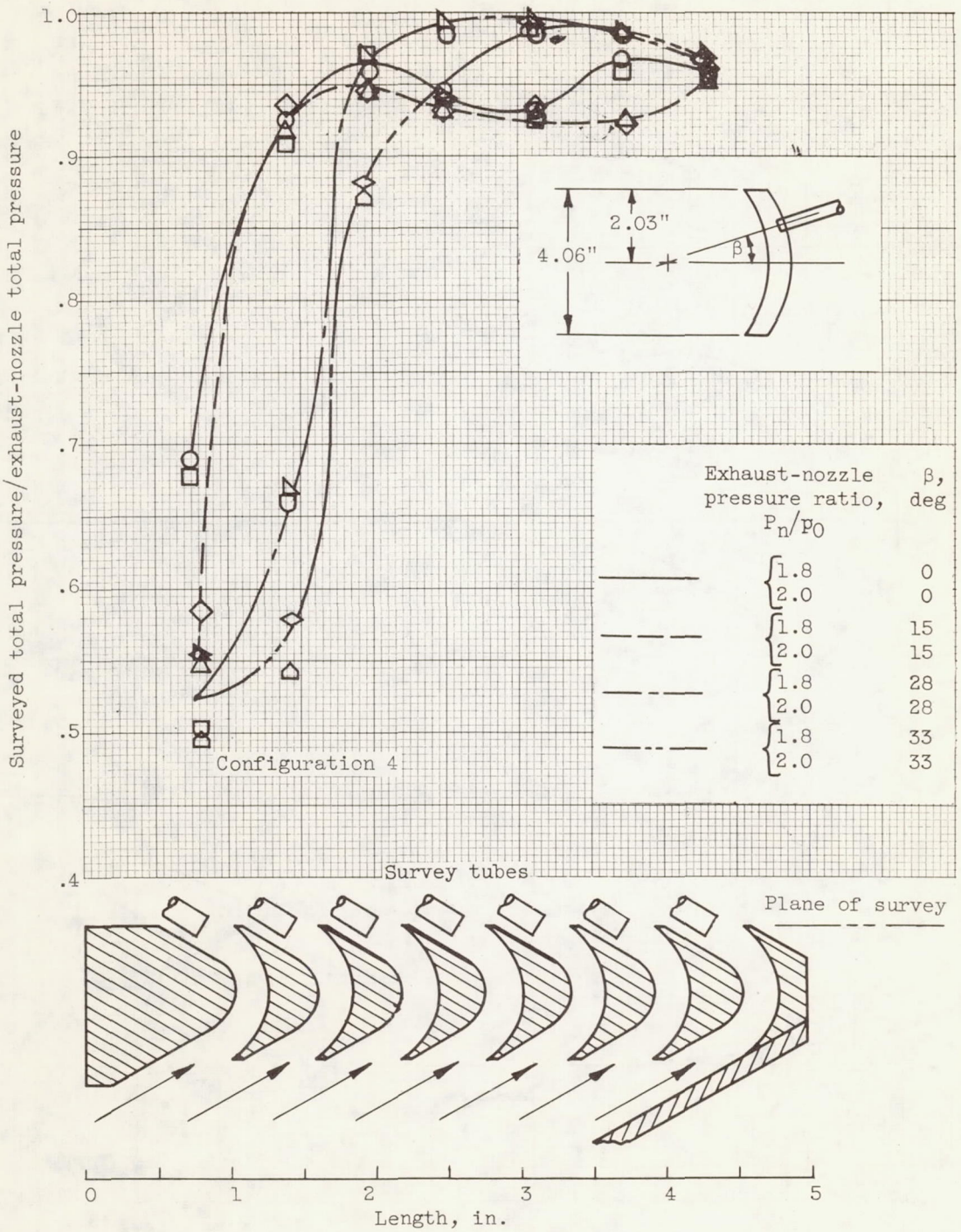

Figure 11. - Total-pressure surveys at the discharge of tail-pipe-cascade-type thrust reverser. Cascade solidity, 1.55; symmetrical, double-curvature blades; full reversal.

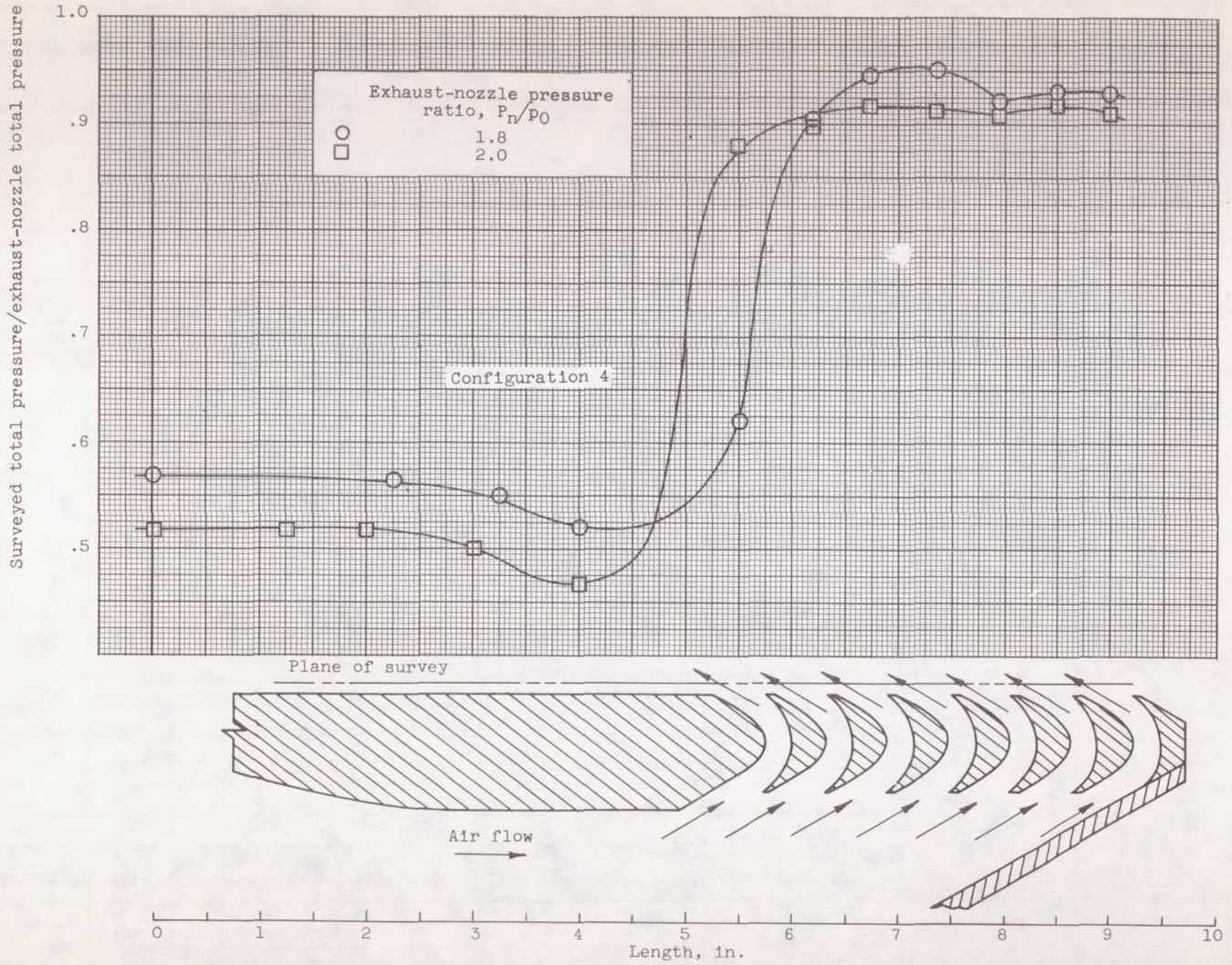

Figure 12. - Total-pressure surveys at the discharge of tail-pipe-cascade-type thrust reverser at various positions parallel to reverser axis. Cascade solidity, 1.55; symmetrical double-curvature blades; full reversal.

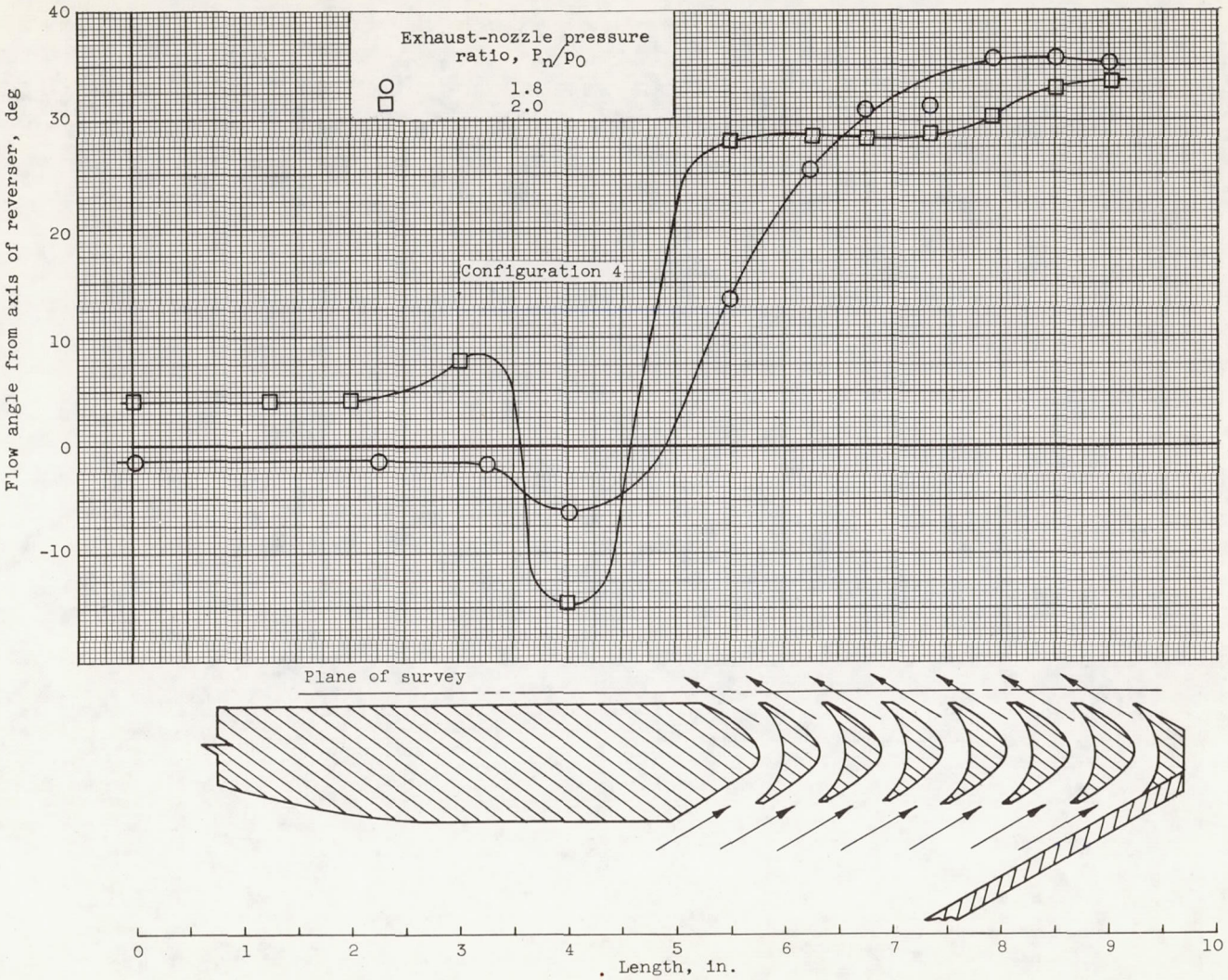

Figure 13. - Flow-angle surveys at the discharge of tail-pipe-cascade-type thrust reverser at various positions parallel to reverser axis. Cascade solidity, 1.55; symmetrical, double-curvature blades; full reversal.

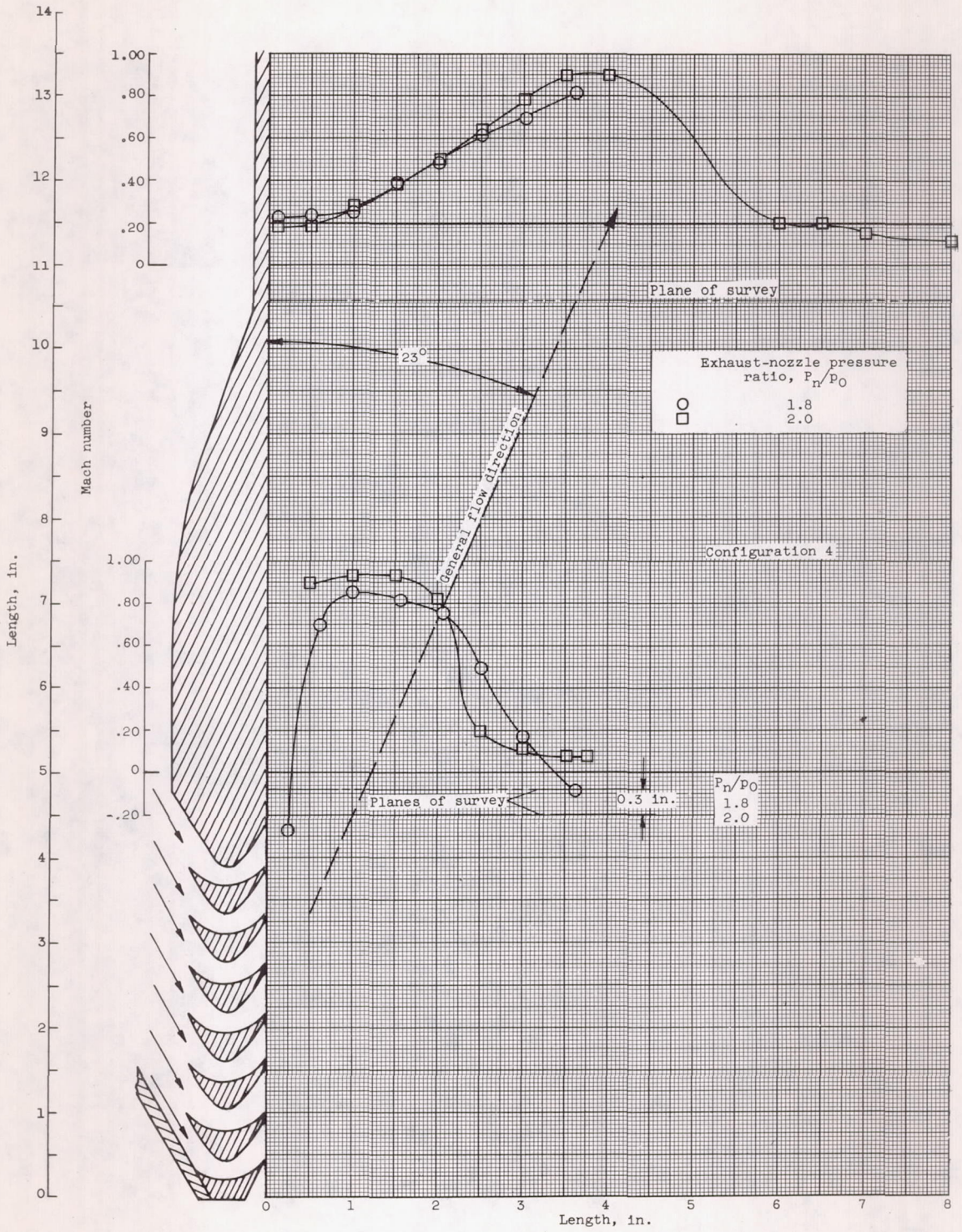

Figure 14. - Mach number surveys outside the discharge of tail-pipe-cascade-type thrust reverser perpendicular to reverser axis. Cascade solidity, 1.55; symmetrical blades; full reversal.

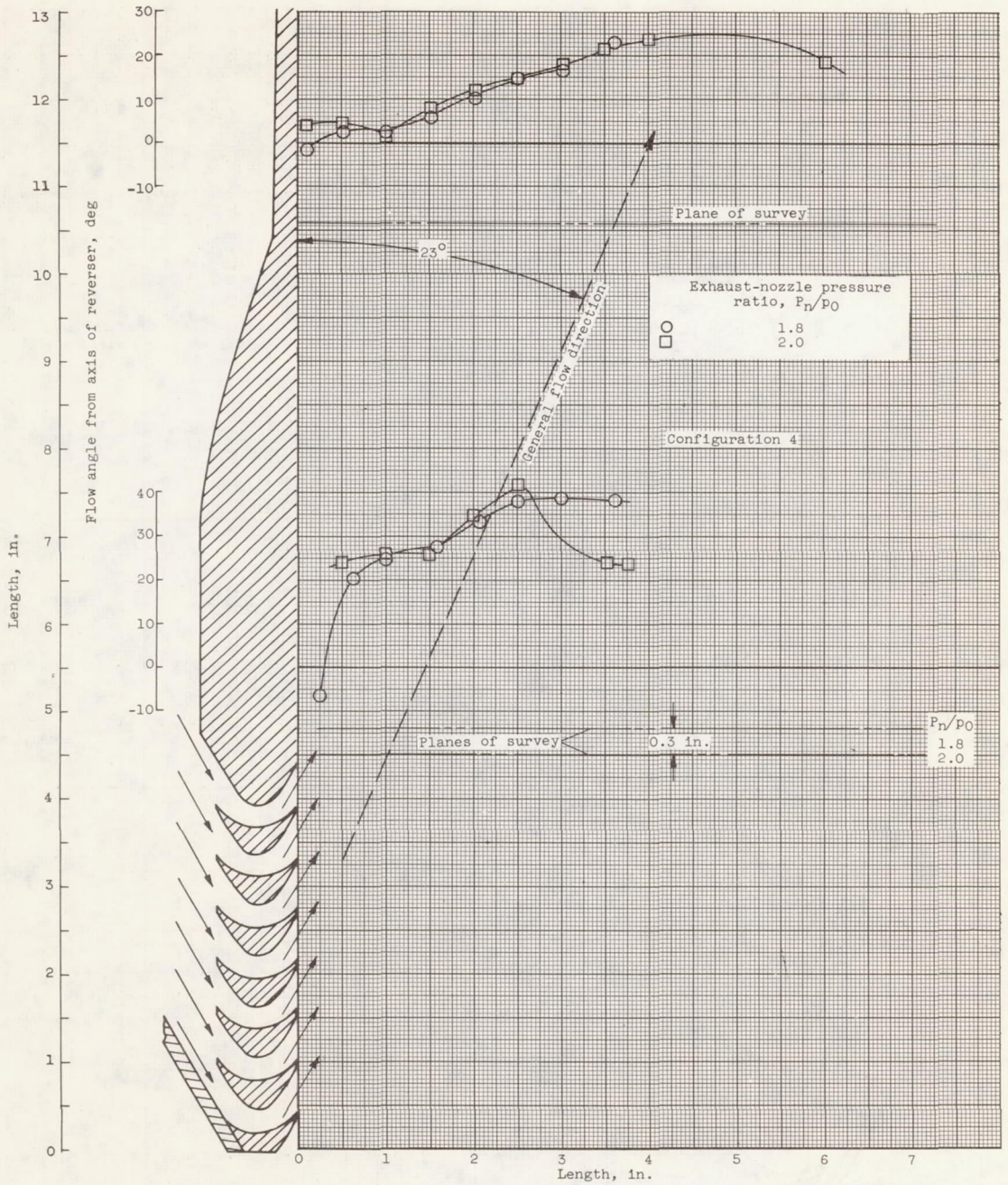

Figure 15. - Flow-angle surveys outside the discharge of tail-pipe-cascade-type thrust reverser perpendicular to reverser axis. Cascade solidity, 1.55; symmetrical blades; full reversal.

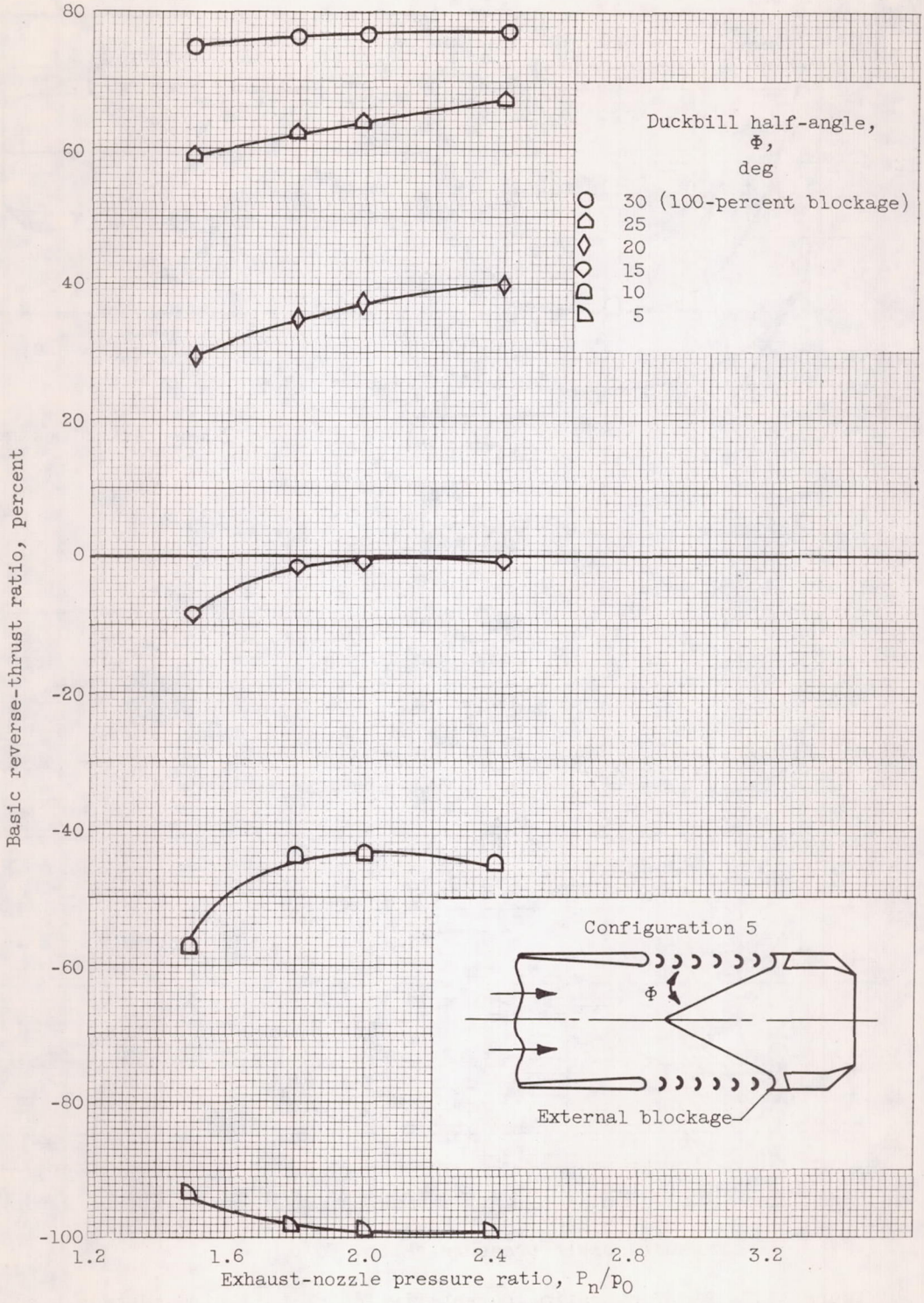

Figure 16. - Thrust-reversal characteristics of tail-pipe-cascade-type thrust reverser at various duckbill half-angles over range of exhaust-nozzle pressure ratios. Cascade solidity, 1.55; symmetrical blades; external blockage.

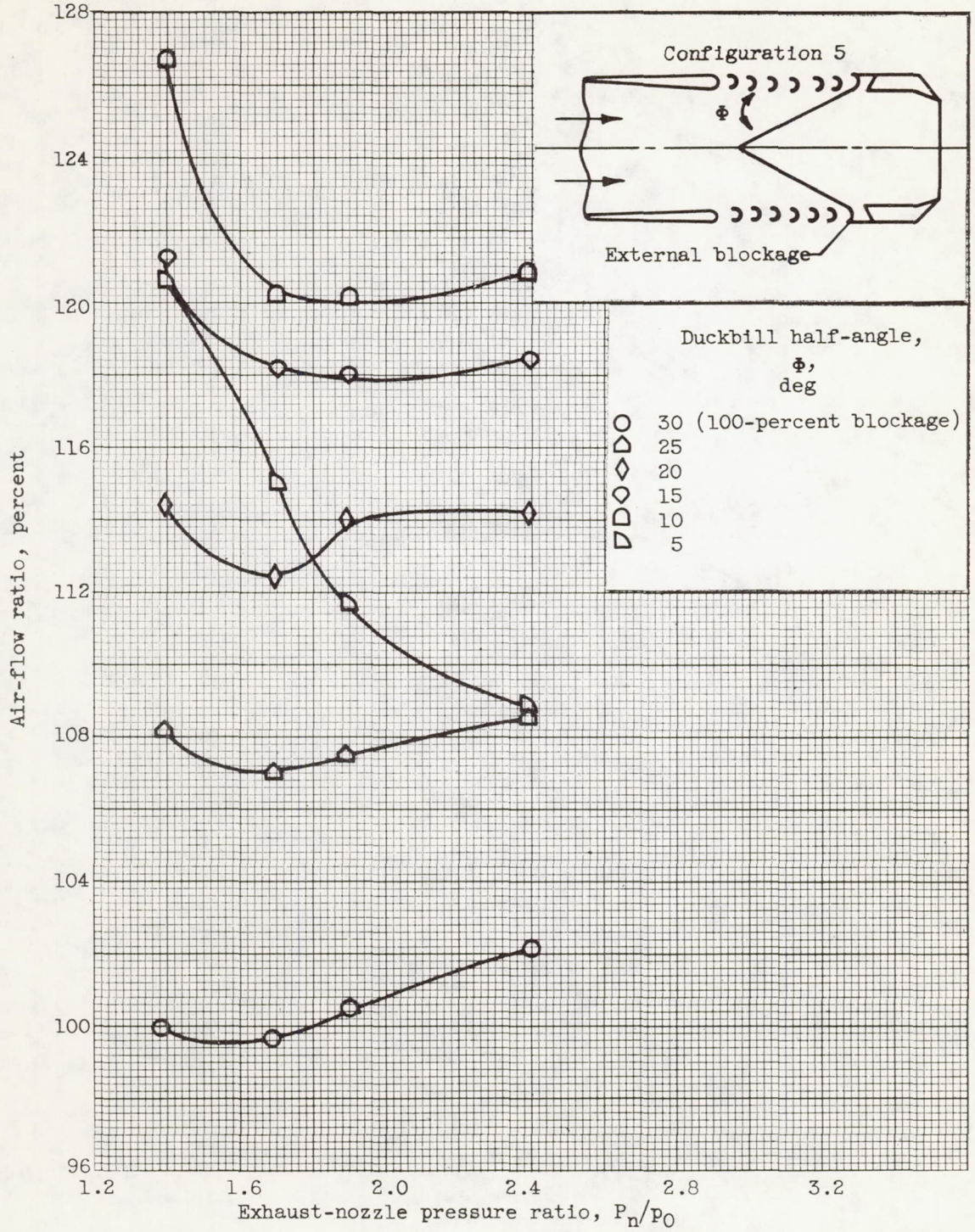

Figure 17. - Air-flow-ratio characteristics of tail-pipe-cascade-type thrust reverser at various duckbill half-angles over range of exhaust-nozzle pressure ratios. Cascade solidity, 1.55; symmetrical blades; external blockage.

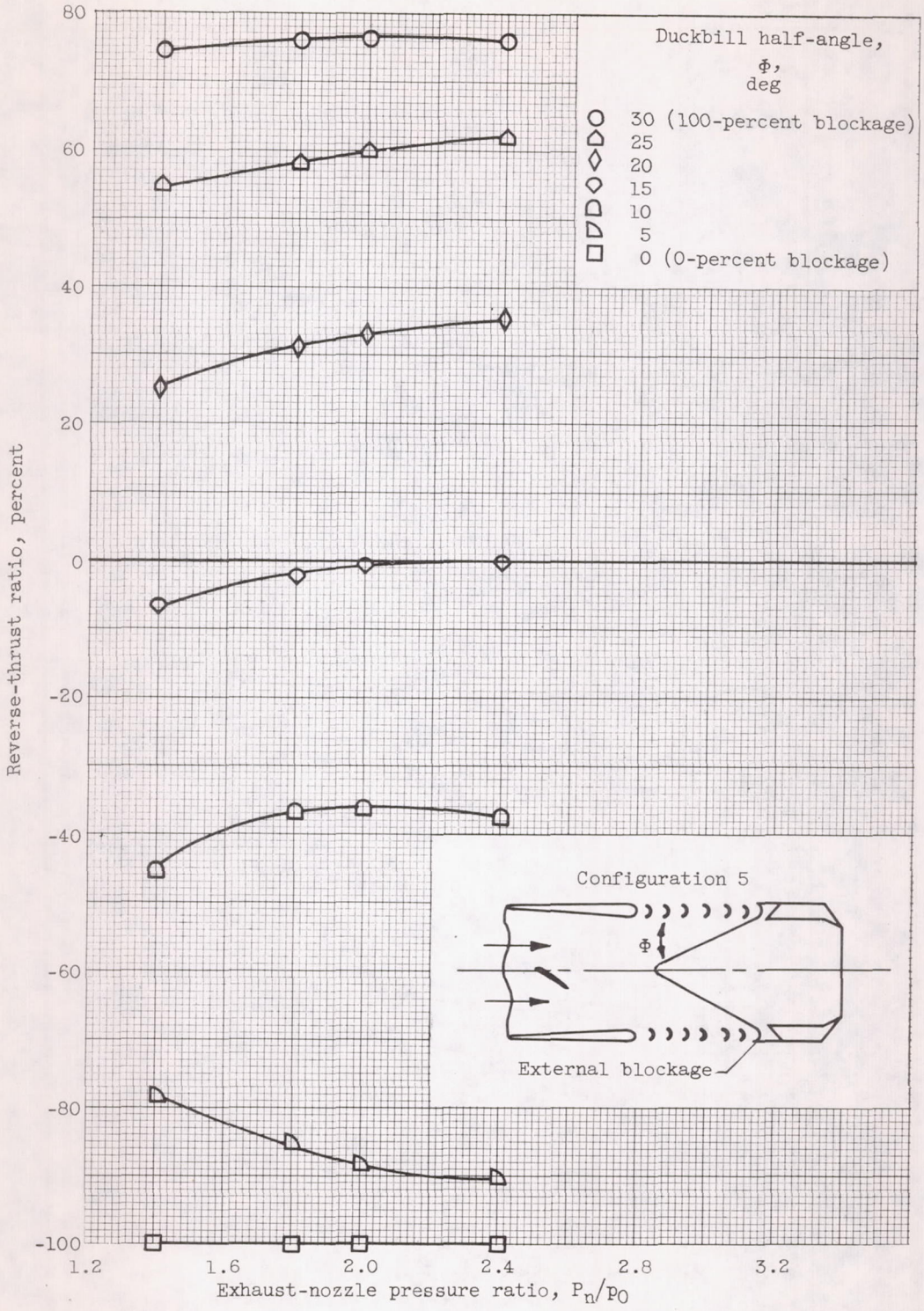

Figure 18. - Reverse-thrust ratio characteristics of tail-pipe-cascade-type thrust reverser at various duckbill half-angles over range of exhaust-nozzle pressure ratios. Cascade solidity, 1.55; symmetrical blades; external blockage.

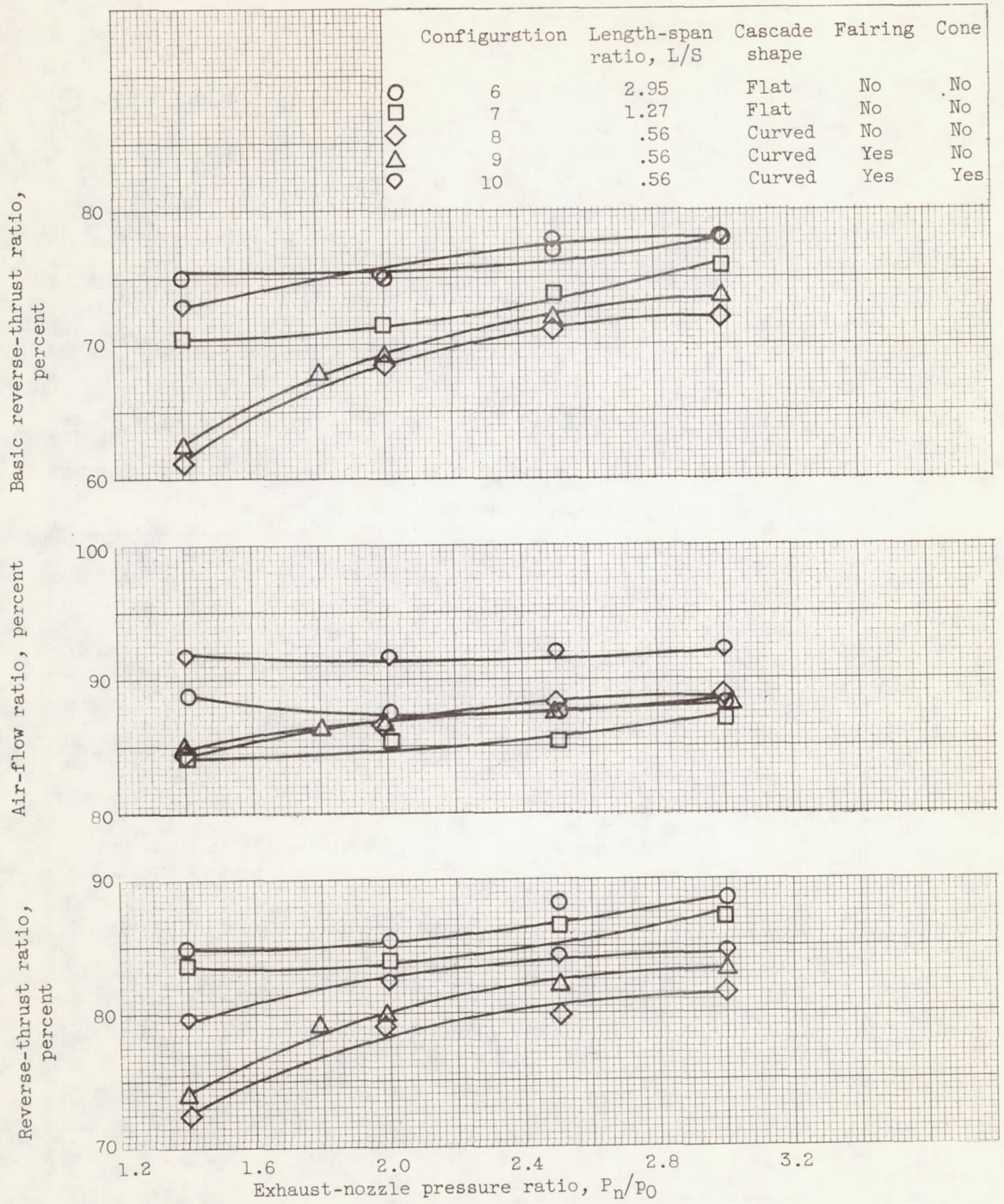

Figure 19. - Air-flow and thrust-reversal characteristics of several tail-pipe-cascade-type thrust reversers over range of exhaust-nozzle pressure ratios, length-to-span ratios, 2.95, 1.27, and 0.61; innerbody length, 18.0 inches; asymmetrical blades; full reversal.

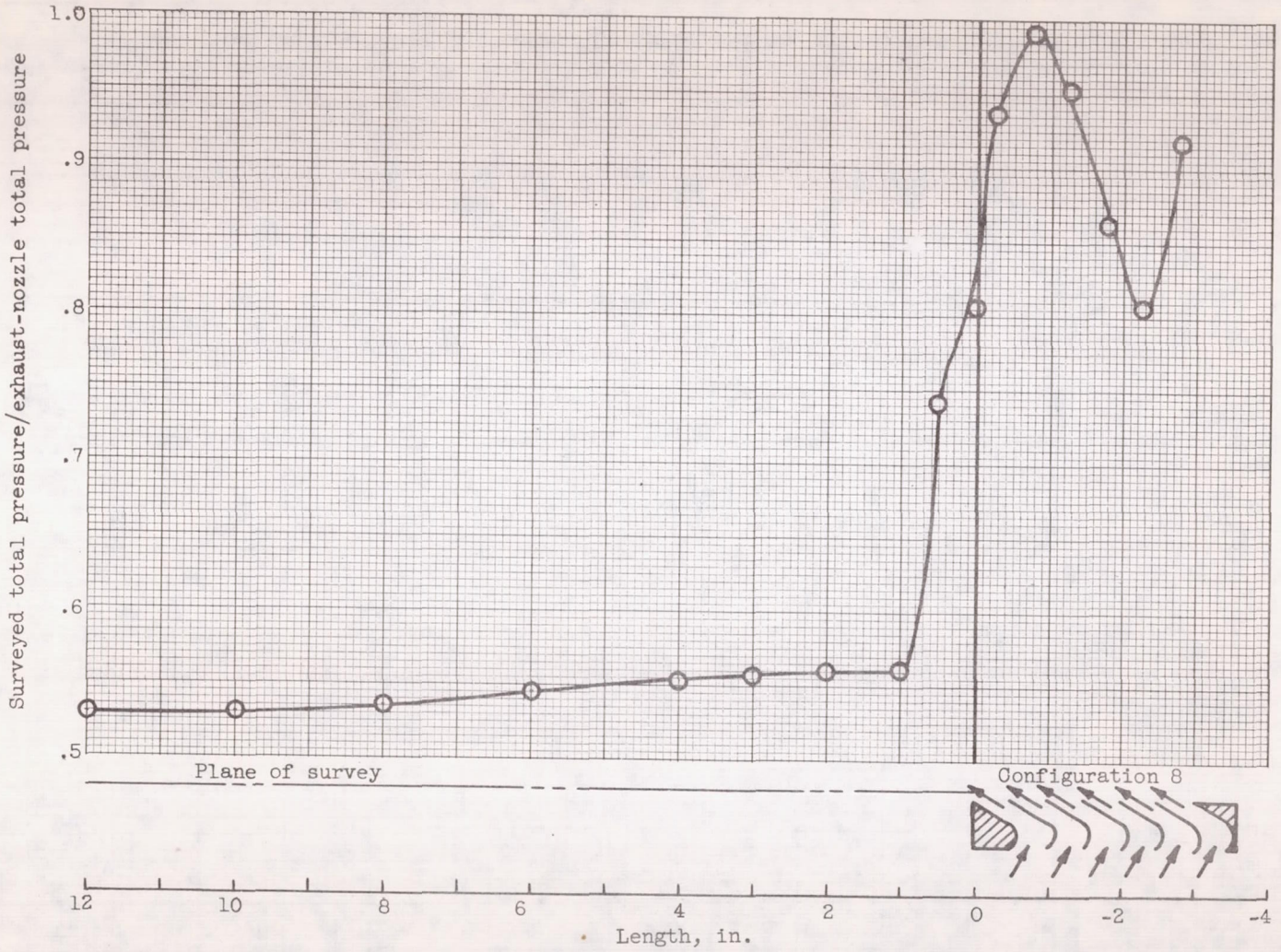

Figure 20. - Total-pressure survey at discharge of tail-pipe-cascade-type thrust reverser at various positions parallel to reverser axis. Length-to-span ratio, 0.56; innerbody length, 18.0 inches; asymmetrical blades; full reversal.

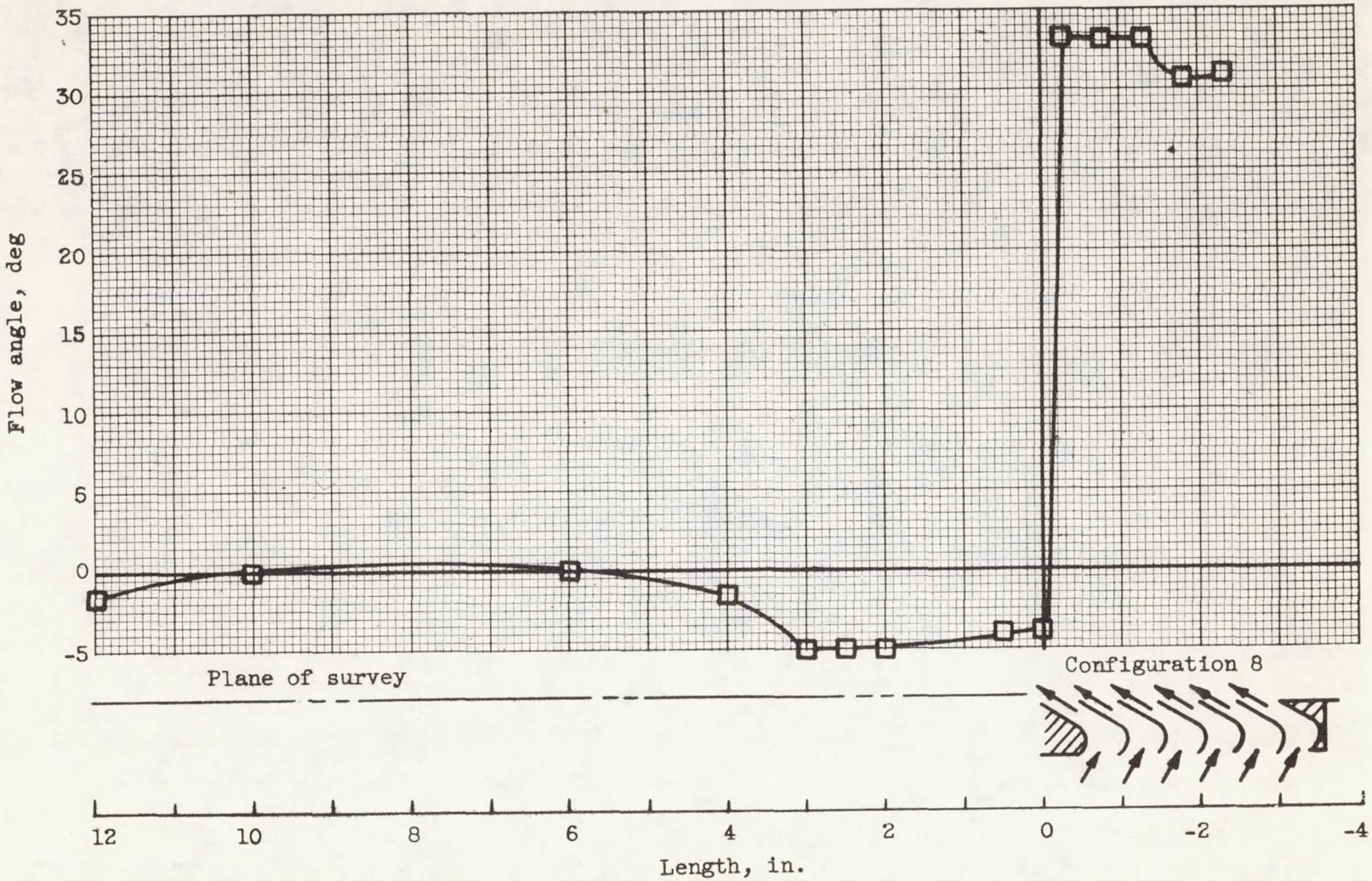

Figure 21. - Flow-angle survey at discharge of tail-pipe-cascade-type thrust reverser at various positions parallel to reverser axis. Length-to-span ratio, 0.56; innerbody length, 18.0 inches; asymmetrical blades; full reversal.

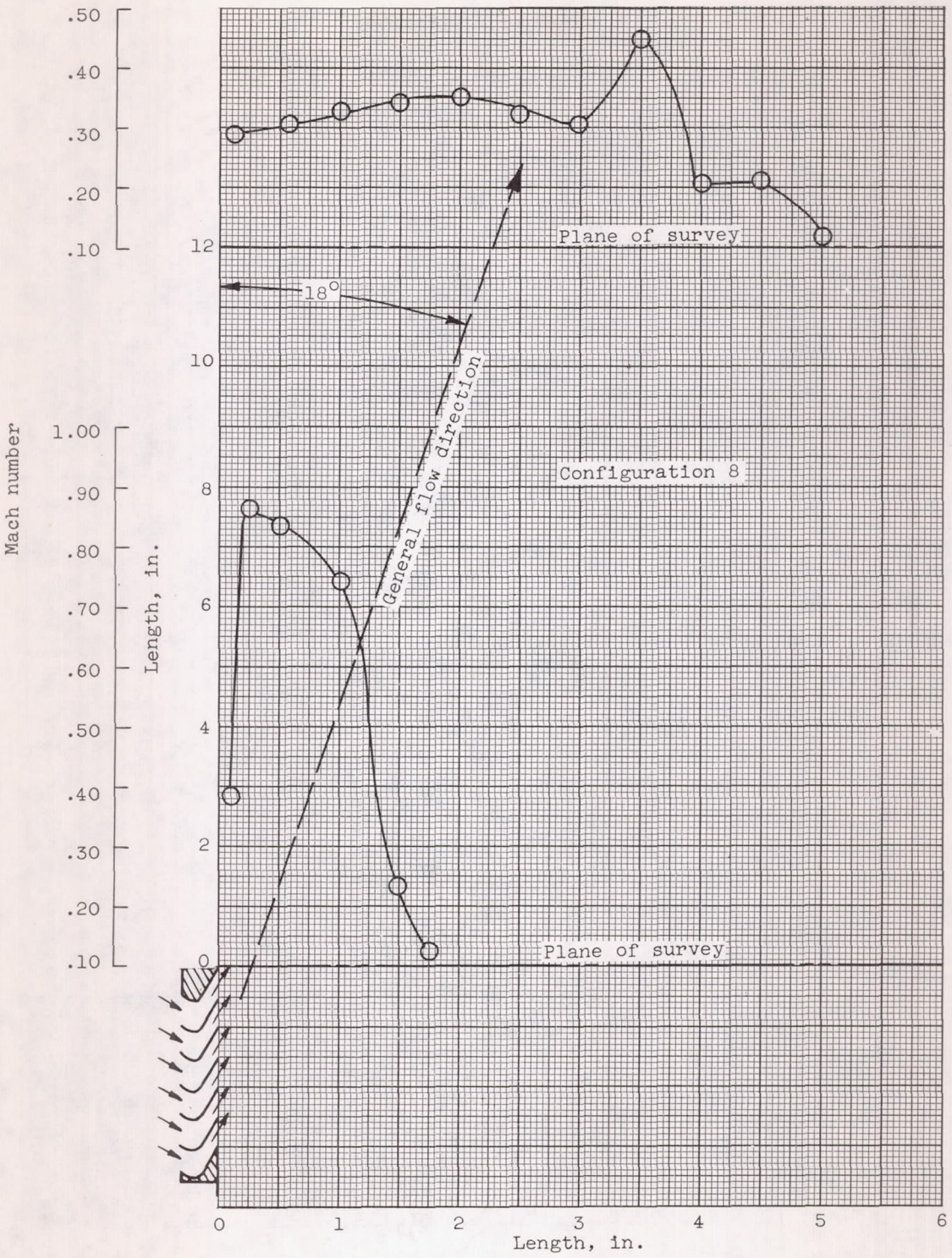

Figure 22. - Mach number surveys outside the discharge of tailpipe-cascade-type thrust reverser at two positions perpendicular to reverser axis. Asymmetrical blades; full reversal.

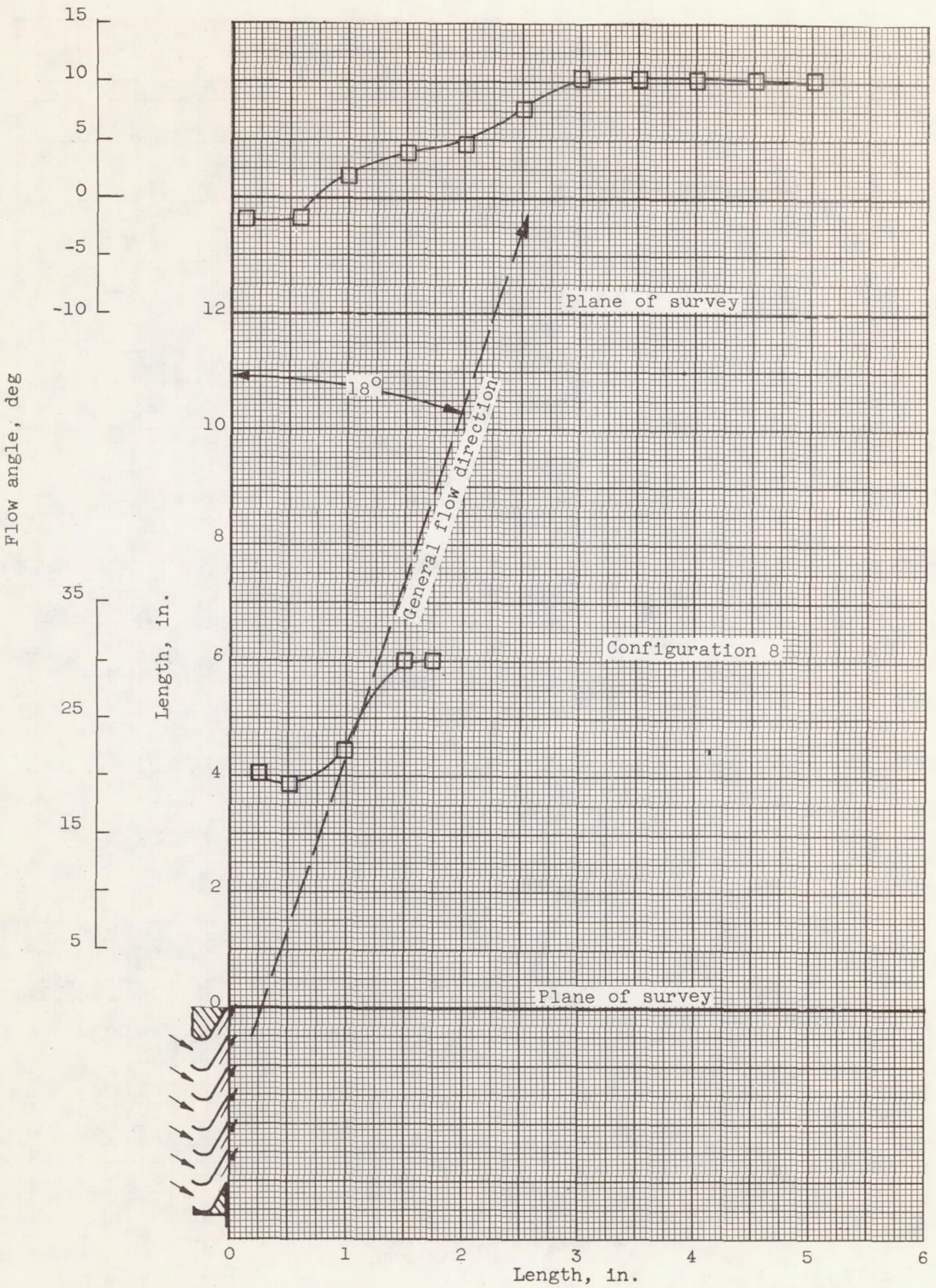

Figure 23. - Flow-angle surveys outside the discharge of tail-pipe-cascade-type thrust reverser at two positions perpendicular to reverser axis. Asymmetrical blades; full reversal.

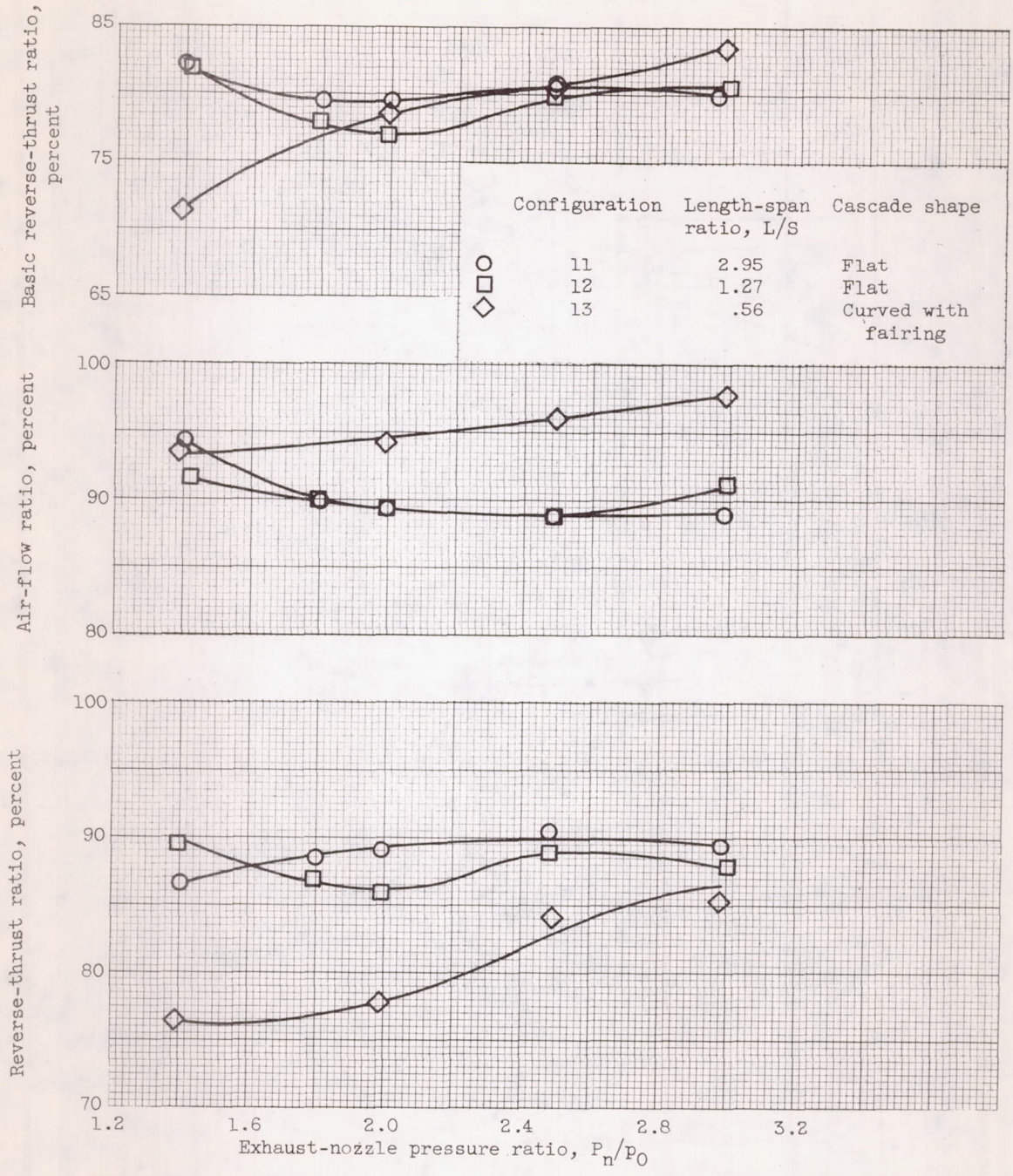

Figure 24. - Air-flow and thrust-reversal characteristics of tail-pipe-cascade-type thrust reverser over range of exhaust-nozzle pressure ratios, length-to-span ratios, 2.95, 1.27, and 0.56; no innerbody; asymmetrical type blading; full reversal.

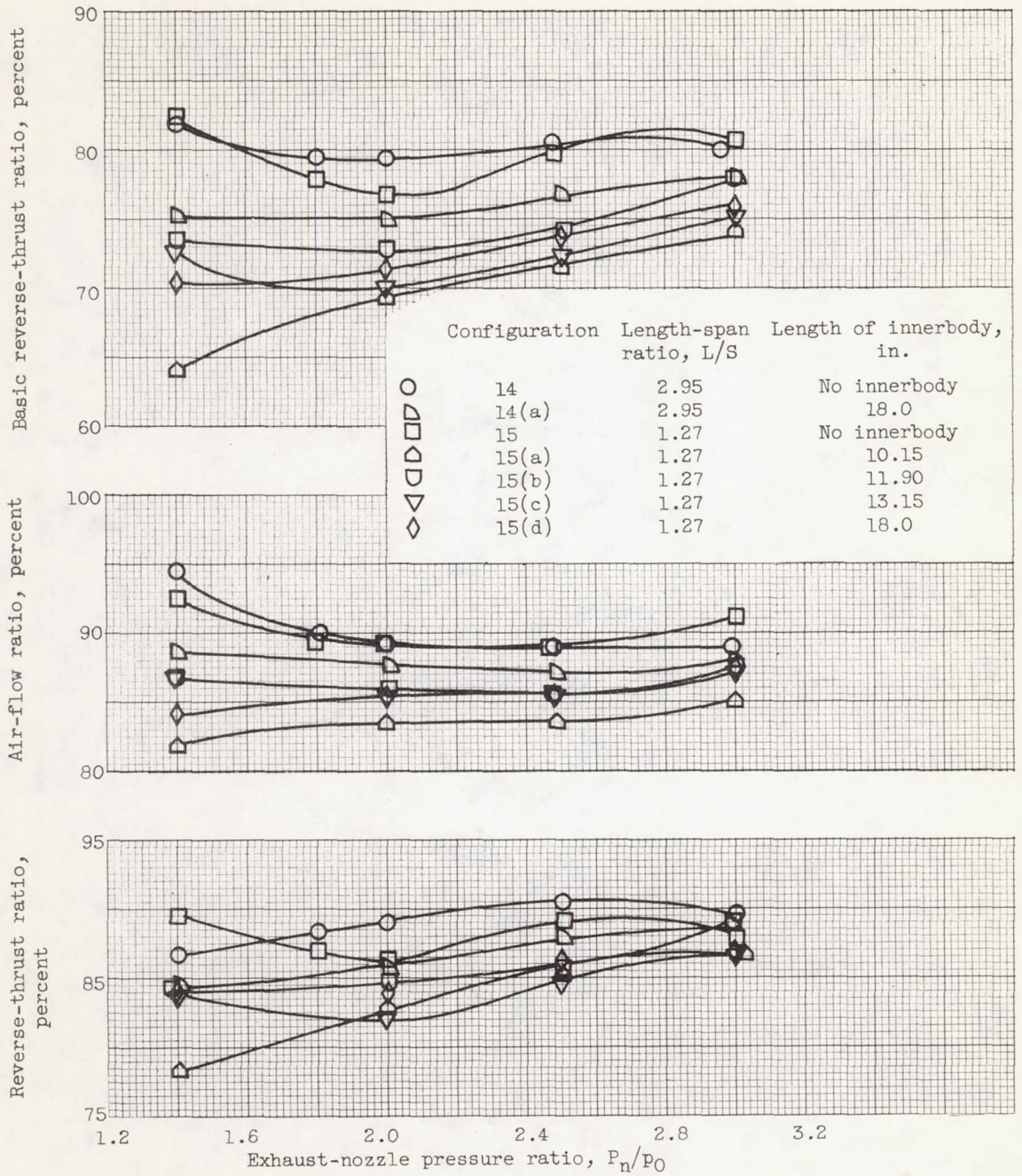

Figure 25. - Air-flow and thrust-reversal characteristics of tail-pipe-cascade-type thrust reverser over range of exhaust-nozzle pressure ratios. Length-to-span ratios, 2.95 and 1.27; various innerbody lengths; asymmetrical blades; full reversal.